A Performance Visualization and Fine-tuning Tool for Arterial Traffic Signal Systems

A THESIS

SUBMITTED TO THE FACULTY OF THE GRADUATE SCHOOL OF THE UNIVERSITY OF MINNESOTA

BY

Jianfeng Zheng

IN PARTIAL FULFILLMENT OF THE REQUIREMENTS FOR THE DEGREE OF MASTER OF SCIENCE

Henry X. Liu (Adviser)

April 2014

ACKNOWLEDGEMENTS

I would like to express my sincere gratitude to my adviser, Prof. Henry X. Liu, for his constant support, patient guidance and many constructive suggestions throughout this research. I would also like to thank Prof. Gary Davis and Prof. Zongxuan Sun, for taking interests in this research and serving in my committees. Many courses from Prof. Gary Davis were greatly beneficial and inspiring for me.

My special thanks go to my fellow colleagues in Prof. Liu's research group, in particular, Dr. Heng Hu, Mr. Jie Sun, Dr. Xinkai Wu from Cal Poly Pomona, for many advices and assistances. Special thanks also go to Mr. Steve Misgen, Mr. Timothy Bangsund and Mr. Curt Krohn for assistance with field implementations of the data collection units. Mr. Kevin Schwartz and Mrs. Nicole Flint also helped with the field experiments for offset changes. Their helps are also acknowledged.

Last but not least, my gratitude goes to the unconditional love and supports from my families, my parents, Mr. Quanshun Zheng and Mrs. Zhujiao Lin, my sisters, Mrs. Surong Zheng and Mrs. Suting Zheng. My gratitude and love to my fiancée, Miss Hanyue Li, who walked all the way with me for past 6 years, are beyond words.

A Performance Visualization and Fine-tuning Tool for Arterial Traffic Signal Systems

By Jianfeng Zheng

ABSTRACT

Maintaining an efficient traffic signal operation is a challenging task for many traffic management agencies. Due to the intensive labor cost required, most of the traffic signals in the US are retimed once every 2-5 years. However, it has been shown in the past that traffic delay increases 3-5% per year simply because the timing plans are not kept up to date. For many resource-constrained agencies, it would be desirable to reduce the signal re-timing costs by automating all or portion of the manual process. The research makes one-step forward towards this direction. In this research, we developed a performance monitoring and visualization tool for arterial traffic signal systems, aiming at reducing the labor cost for signal retiming, and helping to identify signal parameter adjustment opportunities. Specifically, an automated data collection unit (DCU) was developed to collect high-resolution event-based data from signal controller cabinets. Using the high-resolution data, two parameter fine-tuning algorithms were proposed, one for offset and another for green splits. To fine-tune signal offsets, a practical procedure to construct the time space diagram (TS-Diagram) to visualize the progression quality on arterials was proposed. The TS-Diagram was calibrated and validated using the field data collected from the DCUs and the probe vehicle runs. Reasonable agreements between the field observations and the generated TS-Diagrams were found. A field experiment was then carried out, to illustrate how decisions of changes could be made by intuitively evaluating the TS-Diagram. For green splits, an adjusted measure of effectiveness (MOE), the utilized green time (UGT), was proposed for performance evaluation. The information was further tabulated in the form of ring-and-barrier diagram to facilitate evaluation. Field examples were also illustrated to demonstrate implementation potentials for green split evaluation and fine-tuning.

Keywords: Traffic signal operation, High-resolution data collection, Performance evaluation, Data visualization, Arterial coordination, Fine-tuning.

TABLE OF CONTENTS

LIST OF FIGURES

LIST OF TABLES

CHAPTER 1 INTRODUCTION

1.1 Research Motivation

Maintaining an efficient traffic signal operation is a challenging task for many traffic management agencies. In the current state-of-the-practice, the design and update of traffic signal timing parameters, the so-called signal retiming, are mostly based on data collected manually from the field. During the retiming process, the updated signal timing needs to be validated by field observations and minor changes would be made if a discrepancy is observed. Such process is time-consuming and costly. Due to the intensive labor cost involved, most of the traffic signals in the U.S. are only retimed every 2-5 years, despite of a high benefit/cost ratio of 40:1 (Gordon, 2010). Under such circumstances, it is not surprising to see an overall D+ grade for traffic signal systems from the 2012 National Traffic Signal Operation Self-Assessment Survey, as shown in **Figure 1.1**. As indicated in National Transportation Operations Coalition (2012), "improvement and investment in traffic signal operations remain critical".

Figure 1.1 2012 National Traffic Signal Report Card

[Source: National Transportation Operations Coalition, 2012]

Currently, many intersections in the U.S. are operated with vehicle-actuated

signal controller using different vehicle detection systems installed in the field. However, few agencies have archived or analyzed the operational data from the existing signal control systems to improve signal operation. One of the main impediments is that traditional signal controllers normally aggregate data into 5-60 minutes bins, which is unsuitable for performance evaluation of traffic signal system (Liu et al., 2008). Moreover, without standardized data logging and aggregation capability, it is rather inconvenient and difficult for the engineers to access the data within the controllers.

To improve traffic signal operation, researchers in the University of Minnesota have developed the SMART-SIGNAL (Systematic Monitoring of Arterial Road Traffic and Signals) system, for the purpose of performance monitoring of arterial traffic signal system (Liu et al., 2009). The SMART-SIGNAL system can automatically collect high-resolution event-based traffic data at signalized intersections and generate real-time performance measures e.g. queue length and travel time. However, implementation issue exists for the SMART-SIGNAL system to interface with NEMA (National Electrical Manufacturers Association) TS2 cabinets using the SDLC (Synchronous Data Link Control) interface (Liu et al., 2012). More importantly, even though the algorithms to estimate various performance measures have been developed in previous researches (Liu et al., 2008; Liu et al., 2009; Liu & Ma., 2009), how to utilize the archived data to readily fine-tune the traffic signal system has not been addressed yet. This study attempts to fill in these gaps.

1.2 Thesis Summary and Contribution

In this research, we further develop for the SMART-SIGNAL system, with a focus on the development of a systematic fine-tuning tool for the arterial traffic signal system. Our goal is to provide a convenient tool to assist agency engineers to evaluate and fine-tune the arterial traffic signal systems, thus to maintain efficient signal operations. The objective of the fine-tuning tool is twofold: first, to reduce the efforts for manual validation and fine-tuning during the signal retiming process; second, to assist traffic engineers to identify adjustment opportunities over time.

In addition, to address the technical issue with data collection, two types of data collection units (DCUs) are developed based on embedded system technology, to

interface with existing traffic signal cabinets. Building on high performance microcontrollers, the newly developed DCUs are compact and easy-to-install in the field, and thus could serve as a cost-effective and vendor independent solution for agencies to collect high-resolution event-based traffic data.

Based on the event-based data, two modules are proposed for performance visualization and fine-tuning of offsets and green splits respectively. For offsets, we propose a practical procedure to generate the time-space diagram (TS-Diagram), for visualization and evaluation of the progression quality for two-way coordinated arterials. For green splits, an adjusted measure of effectiveness (MOE) extended from queue service time (QST), the utilized green time (UGT), is proposed for performance evaluation. The ring-and-barrier diagram is adopted to tabulate the information, in order to facilitate evaluation.

1.3 Organization of This Thesis

The rest of the thesis is organized as follows: A brief review of the research background and relevant works are stated in Chapter 2. Chapter 3 describes the system architecture of the tool, as well as the details of the development of the DCUs. Chapter 4 introduces the offset fine-tuning module, with a focus on generating the TS-Diagram. The validation of the TS-Diagram, and illustration of fine-tuning application are described as well. The split fine-tuning module is described in Chapter 5. Finally, the concluding remarks and future research directions are summarized in Chapter 6.

CHAPTER 2 BACKGROUND AND RELEVANT WORK

This chapter will start with a brief introduction of traffic signal control. Then, relevant research works regarding data collection and signal optimization will be reviewed.

2.1 Traffic Signal Control at Intersections

To set the stage, we introduce briefly the NEMA ring-and-barrier signal controller, which are widely used throughout the U.S. For more details, we refer to (Koonce et al., 2008).

The NEMA signal controllers operate a sequence of signal phases in a repetitive manner to assign right-of-way to different traffic movements. The operation and setting of the controller are typically tabulated in the ring-and-barrier diagram, showing the phase sequence , movement direction, and green durations for different signal phases. One illustration for a typical four-arm intersection is shown in **Figure 2.1**.

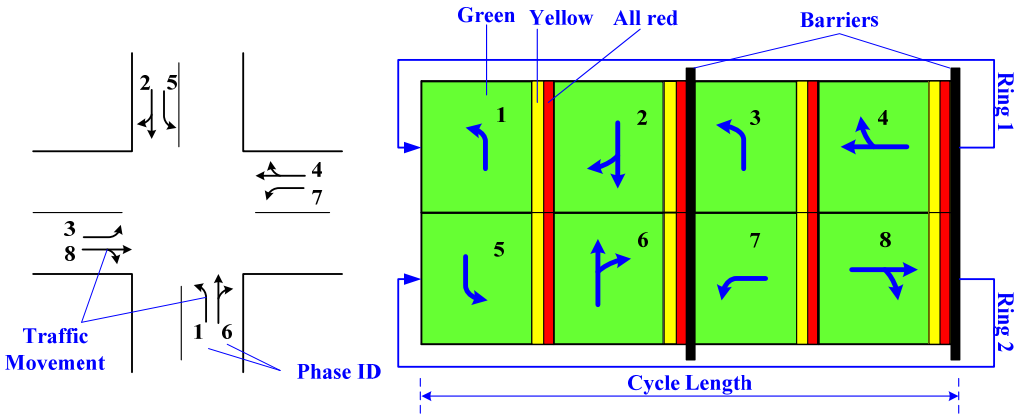

Figure 2.1 Typical intersection layout (left) and ring-and-barrier diagram (right) at a typical four-arm intersection

[Reproduced from: Signal Timing Manual, 2008]

In the example intersection, there are eight traffic movements, controlled by signals with associated signal phase numbers from one to eight. Two rings and barriers are featured in the ring-and-barrier diagram, with phases 1-4 in ring 1 and phases 5-8 in the ring 2. Phases on the two rings are executed concurrently, under certain restrictions: any two phases on the same ring are associated with two conflict movements and cannot

be in green concurrently, so as for any two phases in different sides of the barriers. For each phase, the duration intervals for green, yellow, and red clearance signal are assigned, with the sum as the *phase duration*. The controller will execute each phase based on its order on the ring repeatedly. Every one complete sequence of all phases is called a *cycle*, with the time elapsed during a cycle as the *cycle length*. The percentage of a cycle length allocated as a green phase is the *green split* of the phase. Because of the cyclic operation, there are typically two clocks running in a controller, the system clock tracking the time of day, and a cycle clock tracking the time within a cycle.

Depending on different types of signal controls, the phase duration can be also different. Due to safety concerns, the yellow time and red clearance time are typically fixed regardless of control mode. The green time of each phase is constant for fixed signal, but could be different from cycle to cycle for actuated control, in response to the detector actuations.

On arterials, coordinated-actuated control is normally deployed, with two through movements on the major road prioritized by the coordinated phases, phase 2 and phase 6 by convention. The coordinated phases will be synchronized with a specified reference point to facilitate vehicle platoon progression on the main road. To maintain the synchronization, the cycle length will be fixed for each intersection and a common cycle length will be shared by several adjacent intersections. Typically, a master intersection is indicated, running a master cycle clock. The rest of the intersections will run local cycle clock individually, with a specified shift from the master cycle clock. The difference between a local cycle clock with the master cycle clock, given a specified reference point, is the *offset* of the intersection.

One illustration of the offsets is shown in **Figure 2.2,** with the green end of the coordinated phase as the reference point. The intersection (Int.) B is the master intersection, and local clock at Int. A is shifted with 30 sec to the right from the master clock at Int. B. Accordingly, the offset of Int. B is 0 sec, and offset of Int. A will be 30 sec.

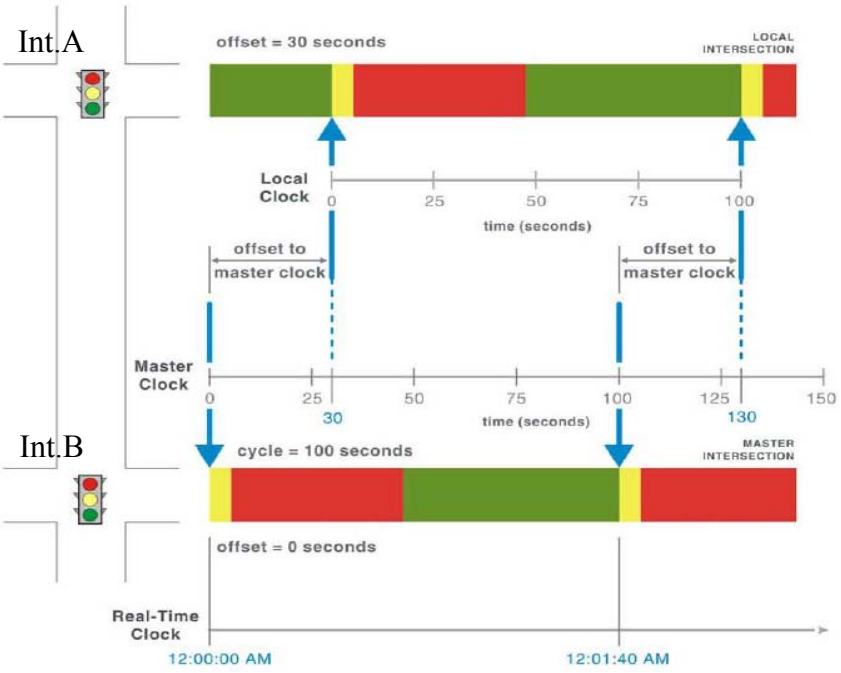

Figure 2.2 Illustration of Offset

[Source: Signal Timing Manual, 2008]

To keep a fixed cycle length for the coordinated actuated control, only some of the phases are vehicle-actuated. One common choice is to set the non-coordinated phases as actuated, with coordinated phases as non-actuated. Thus, the unused green time of the non-coordinated phases will revert to the coordinated phases. Vice versa, the coordinated phases can be also set as actuated, with non-coordinated phases as non-actuated, and the unused green time of coordinated phases will revert to non-coordinated phases.

2.2 Data Collection for Signalized Intersections

While real-time performance measures for freeway are commonly available in the forms of speeds and travel time nowadays, they are relatively new for signalized intersections (Day et al., 2010a). According to 2012 National Traffic Signal Operation Self-Assessment Survey, arterial data collection remains at F grade from 2007 to 2012, showing significant needs and potentials for improvements (National Transportation Operations Coalition, 2012).

In general, many existing controllers for traditional traffic signal systems have the capability to generate basic measure of effectiveness (MOE) reports. For instance, Eagle® EPAC 300 controller can generate MOE reports with volume, stops, delays and utilization of green time (Balke et al., 2005). Volume, occupancy and average speed (if speed detectors are available) aggregated in 5-60 minutes can be also obtained from Econolite ASC/3 family controller (Econolite ASC/3 Controller Specification, 2012). However, the MOEs generated within controller have not been standardized yet, and is not utilized by most of the engineers operating the traffic system (Balke & Herrick, 2004; Balke et al., 2005).

One of noteworthy work of data collection system for signalized network is the Arterial Performance Measurement Systems (A-PeMS) developed by University of California, Berkeley in cooperation with the Los Angeles Department of Transportation (Petty et al., 2005). A-PeMS aggregates traffic volume and occupancy data in 30-second intervals, and can generate performance measures such as link travel time and intersection delays.

Recently, emerging interests can be found in using high resolution event-based data for performance measure of the traffic signal system, and encouraging results were achieved (Smaglik et al., 2007; Day et al., 2009; Day et al., 2010a; Day et al., 2010b; Liu & Ma, 2009; Liu et al., 2009; Wu et al., 2010). The "events" here are referred as vehicle-detector actuation and de-actuation, as wells as traffic signal phase changes, all in high-resolution time intervals. The advantages of the event-based data over aggregated data are: (a) performance indexes based on large (hour or day) or medium time interval (phase or cycle) can be easily calculated and (b) investigation on microscopic level is feasible and could help for more accurate and detailed evaluation, particularly during congested traffic condition.

2.3 Event-based Data Collection

To collect high-resolution event-based traffic data, additional adjustments are needed for most of existing traffic signal systems. Several solutions have been reported so far, whereas there is a lack of solutions that can be readily deployed.

To address the issue of non-standardized interface of controller MOE output, Bullock and Catarella (1998) developed the controller interface device (CID) that can interface signal controller with PC regarding signal events and detector events in real time. With CID, the hardware-in-the-loop simulation (HILS) can be established incorporating traffic controllers from different vendors. Advanced Traffic Analysis Center (ATAC) of North Dakota State University (Smadi & Birst, 2006) has developed CID for NEMA TS2 controllers. Since the CIDs are designed for interfacing controller with simulation package in personal computer, they cannot be used to collect detector data independently.

TTI's TSPMS extends CID with I/O data acquisition card to obtain signal and detector event data from TS1 cabinet. The data is further processed by an industrial computer within cabinet. For TS2 cabinet, they use enhanced BIU by Naztec Inc. to interface with SDLC bus, and the industrial computer is replaced by a rugged laptop for easier user interaction (Balke et al., 2005; Sunkari et al., 2011). This architecture for data collection system for TS1 cabinets is adopted and extended by the first version of the SMART-SIGNAL system.

National Institute for Advanced Transportation Technology (NIATT) in University of Idaho also developed a data logging device for high-resolution event-based data collection, adopting similar architecture of data collection system in TSPMS for TS1 cabinets (Ahmed & Brian, 2008). Although Synchronous Data Link Control (SDLC) interface is recognized, the connection of data logging device for TS2 cabinet is still based on harness cable connecting the connection matrix on the back panel.

One trial version of Econolite Controller Software, Econolite ASC/3 Data Logger, features a logging capability that can retrieve event-based data (Smaglik et al., 2007). Events are recorded with 0.1 sec time stamping, and stored as binary-formatted files. The raw data can be stored within controller for 30 hours, and downloaded via FTP. The data logger is now available within the newly released CENTRACS system (CENTRACS System Datasheet, 2013).

Major limitations of existing solutions can be summarized as: (1) solutions with multiple off-the-shelf components incur unnecessary cost and space within cabinets. It

further increases the difficulty of installation in the field. (2) vender dependent solution e.g. Econolite ASC/3 Data Logger, is far from standardization and is not convenient for agencies with controllers from different vendors. While efforts can seen from vendor side to enhanced event-based data collection within controllers (Duncan, 2011), for a perceived future, the progress for standardization could be gradual and time consuming. This calls for an alternative, vendor independent solution for high resolution event-based data collection.

2.4 Optimization for Traffic Signal System

Since Webster's classical work (Webster, 1952), extensive researches have been dedicated to the optimization of cycle length, split, and offset of a traffic signal system. Many of the well-established methodologies, however, are concentrated on optimization during design stage of signal timing.

Early studies were primarily concentrated on parameter optimization for fixed time signal control. In Webster's seminal work, analytical formulas were derived for split and cycle length optimization for fixed time control at isolated intersections (Webster, 1958). Considering intersections in coordinated networks, Gartner & Little (1975) proposed the generalized combination method, which uses a simplified link based delay calculation to optimize offset, split and cycle length simultaneously. Later, MAXBAND and its derivatives were proposed, in that the offset optimization problem is formulated as a mix integer linear programming (MILP) problem with green bandwidth as the optimization objective (Little et al., 1981; Gartner et al., 1990). Another important work was done by Robertson (1969), in which the platoon dispersion model was developed for more comprehensive estimation of performance index. The platoon dispersion model was then used in the popular signal optimization package TRANSYT, and later adopted in the SCOOT adaptive signal control system (Robertson & Bretherton, 1991).

With increasing implementations of vehicle-actuated controllers, attentions were then paid to optimize the parameters of actuated control. Lin (1982a) proposed models to estimate the average green for fully actuated signals assuming Poisson distribution for the arrivals. The model was further extended to estimate cycle length and green split

for both semi-actuated and fully actuated signal control (Lin, 1982b). Extension of the work can be also found in Akcelik (1994) by assuming M3 model by Cowan (1975) for headway distribution of the arrivals. To convert fixed signal plan to actuated/semi-actuated signal plan, Skabardonis (1996) proposed adjustments with focus on force off, yield point and max green time of the coordinated-actuated signals. The essence of the adjustments is to better estimate the green start and end times of the coordinated phases.

More recently, with the increasing data availability, several researches have been conducted to optimize coordinated-actuated traffic signals based on signal and detector data. For instance, Yin et al (2007) developed an offset refiner utilizing historical signal data only. In addition to bandwidth, the red-meeting probability was proposed as another metric, to minimize the occurrence of early return to green. Based on the similar concept, Zhang and Yin (2008) proposes a robust synchronization approach to extend the MAXBAND with uncertain green start times.

Some other researches intend to investigate signal and detector data jointly. Abbas et al. (2001) introduce the cyclic volume and occupancy profiles and develops a continuous adjustment algorithm for offset transitioning. Based on time-stamped phase and detector state changes collected by a logger in the Econolite ASC/3 controller, Smaglik et al. (2007) demonstrates procedures to calculate popular performance measures such as v/c ratio, arrival types and vehicle delays, for actuated traffic signals. The same type of data is also used in Day et al (2010), which develops a visualization tool, namely the Purdue Coordination Diagram (PCD), for evaluating coordination qualities on arterials. Day & Bullock (2011) further extends the combination method, and propose the link pivoting combination method (LPCM) for offset optimization.

2.5 Summary

Over the past decades, the advances in computer and communication technologies make it feasible to collect and archive massive amount of high-resolution data for the signalized intersections. This is particularly attractive and beneficial for performance monitoring and evaluation, the precursors to effective and efficient operations. While some approaches have been proposed for event-based data collection, a general and readily implementable solution is still lacking. Regarding the optimization of the traffic

signal systems, on one hand, many well-established methods are only suitable in design stage of signal timing, requiring manually collected data. On the other hand, recent approaches either adopt simplified optimization objective e.g. green signal bandwidth, or rely on simplified assumptions that only adjacent intersections are considered, which could fail to address various concerns raised by many associated factors for signal coordination on arterials (Koonce et al., 2008).

In this study, we aim to develop a systematic tool for event-based data collection and performance evaluation and fine-tuning, for signalized arterials. A compact, easy-to-install, and vendor independent data collection unit (DCU) was developed for high-resolution event based data collection. Using event-based data, two modules were developed for fine-tuning of offset and green splits, respectively. Different from previous approaches in the literature that focuses on optimization algorithms, the development of fine-tuning methodologies here was concentrated on visualizing the performance of the arterial traffic signal system. Hence, various concerns for signal timing parameters could be considered and evaluated easily. The details of development and potential applications of the developed tools are presented in the following chapters.

CHAPTER 3 SYSTEM ARCHITECTURE AND DATA COLLECTION UNIT (DCU)

This chapter will describe the system architecture of the tool, followed by the details of the development of the DCUs for high-resolution event-based data collection.

This research is focus on signalized arterials with two through directions coordinated. In the investigated scenarios, we assume that advance detectors are available for detection of through traffic, with the stop bar detectors available for the left turn and side street traffic. This is a simple yet quite common setting for the arterials. An illustration of the setting is shown in **Figure 3.1**

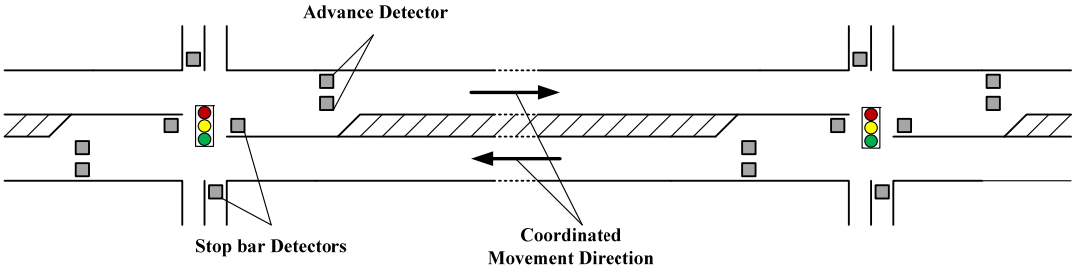

Figure 3.1 Typical layout and detector setting of an arterial

3.1 SYSTEM ARCHITECTURE

For compatibility, the system architecture of the tool is inherited from the SMART-SIGNAL system. This is shown in **Figure 3.2**. The first box indicates the data collection system implemented in the field. Two types of data, the signal events and detector events are collected, stored in log files, and transmitted to the central database, indicated in the second box. Then, evaluation report will be generated in the central server, and will be made available to the traffic engineers. Note that, the tool will serve as a decision support system, while the final change and implementation decisions still need to be made and executed by engineers.

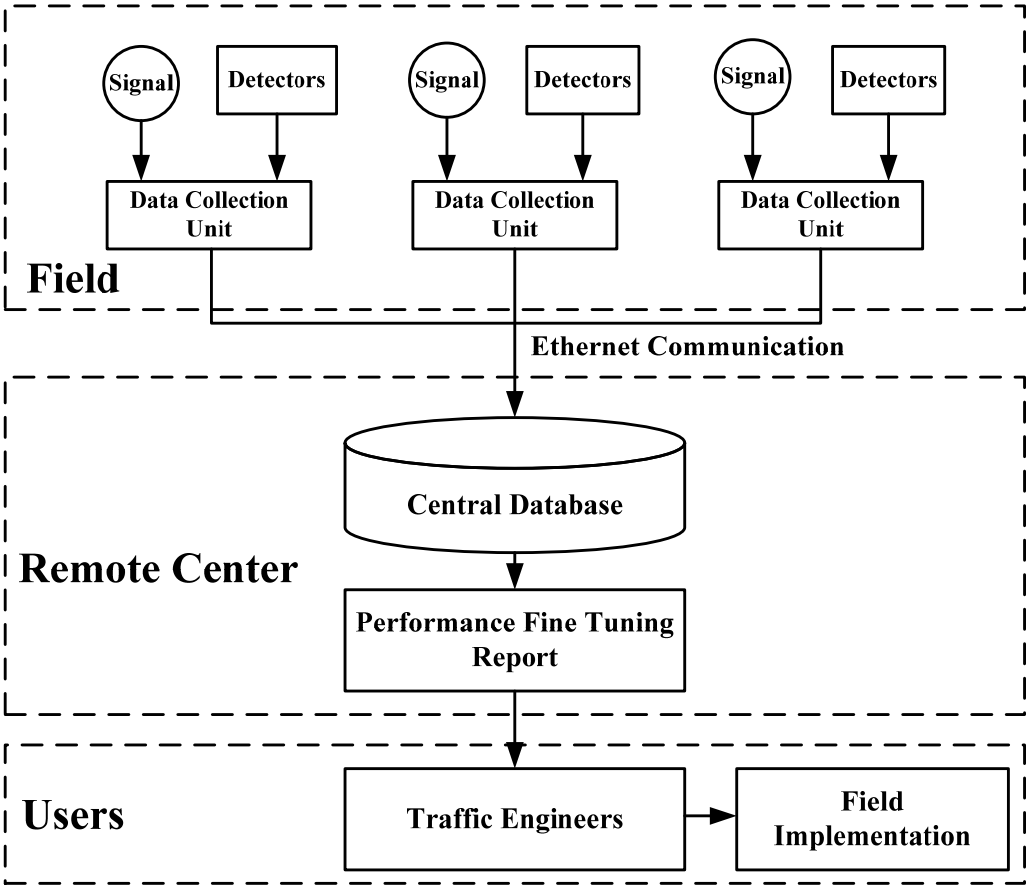

Figure 3.2 System architecture of the fine-tuning tool

[Extended from SMART-SIGNAL System architecture (Liu et al., 2009)]

Two fine-tuning modules are proposed, for offset and splits respectively. While the details of each fine-tuning modules will be described in chapter 4 and 5, the procedures for fine-tuning process are illustrated in **Figure 3.3.** As shown in the figure, the fine-tuning procedure is a periodical and iterative process, with implementation of changes in the field. Additionally, the fine-tuning of green splits and offsets are proposed to be executed in a parallel manner. Since many agencies have special concerns over the progression quality on main road, the proposed fine-tuning of green splits is restricted to non-coordinated phases only, to ensure minimal impact on the progression.

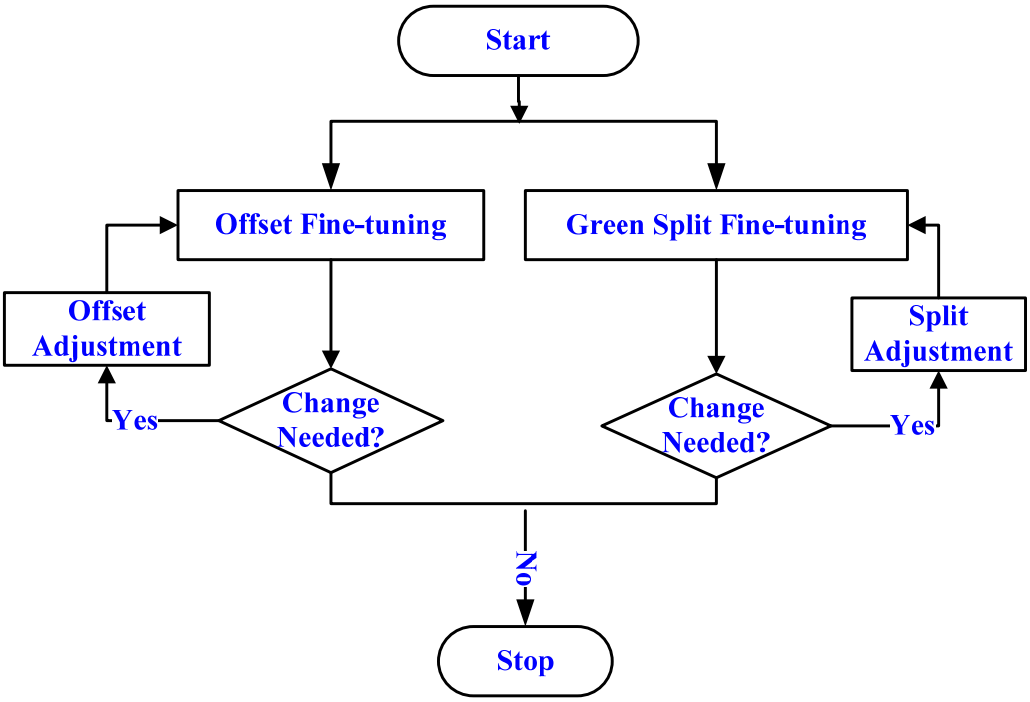

Figure 3.3 Procedure for traffic signal fine-tuning

3.2 Development of Data Collection Unit

The DCUs serve as the units to collect the high-resolution event-based traffic data. **Figure 3.4** illustrates data collection components in the field. Data collection elements include the DCUs in each intersection and a data server in the remote center.

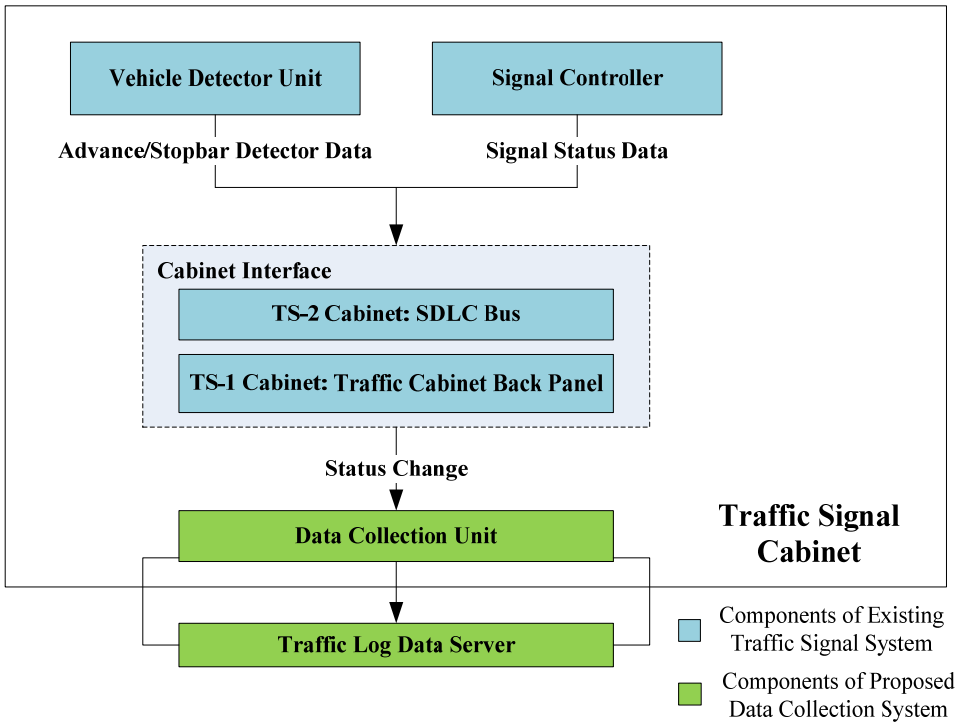

Figure 3.4 Architecture of the traffic data collection components

[Adopted from Balke et al., 2005]

3.2.1 Hardware Design of DCU

Previous development of data collection system in SMART-SIGNAL system is based on the prototype of the TSPMS system, using industrial computer with data acquisition card (Liu et al., 2008). With increasing replacements of NEMA TS1 cabinets by the NEMA TS2 cabinets, compatibility issues occur for the data collection system to interface with SDLC bus in the NEMA TS2 cabinets. The design with multiple components also occupies cumbersome space and further complicates wiring within cabinets. The re-designed DCUs will overcome these issues.

To be compatible with both TS1 and TS2 cabinets, we designed two types of DCUs: TS1 DCU with interface based on contact closures on back panel of the cabinet, and TS2 DCU with interface using SDLC bus. Both types of the DCUs are designed as industrial single board computers, providing media card slot to store log files and an Ethernet port for data transmission. A serial port is also provided for trouble shooting of the DCUs. To avoid interrupting the signal operation, the interfaces of DCUs with the

cabinets are designed to be unidirectional with inputs only, and are not capable to output electrical signals. The architecture of the DCUs is shown in **Figure 3.5,** with snapshots of sample devices.

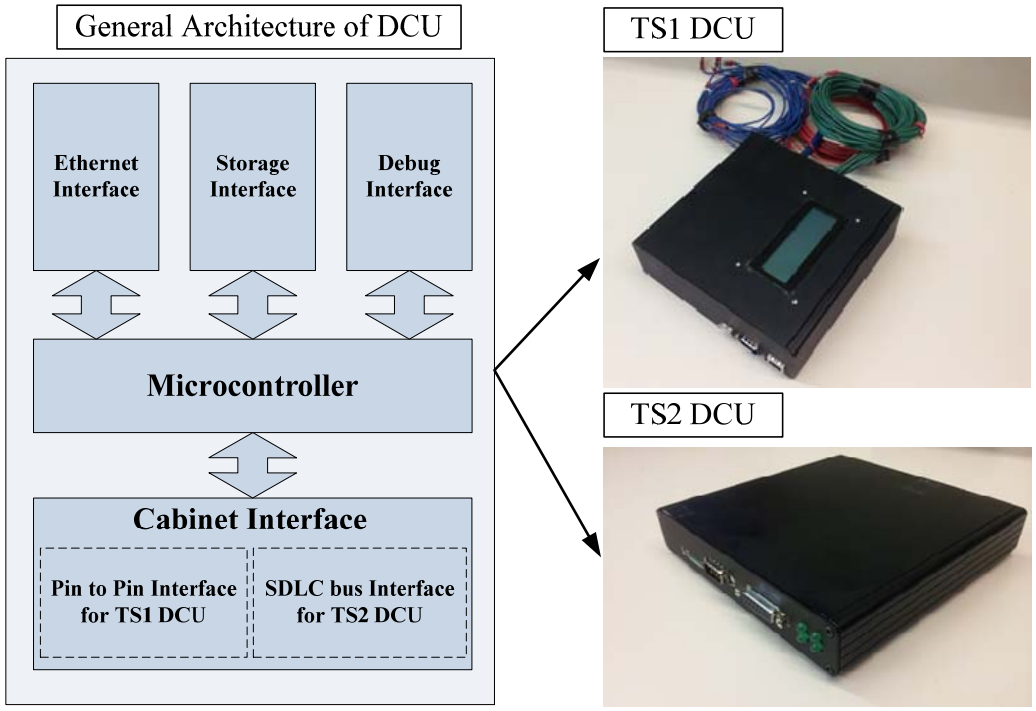

Figure 3.5 General architecture and snapshot of the DCUs

3.2.2 Firmware Design

Data Format

The data regarding every change of detector actuation status and signal status will be recorded and stored. For detector events, the start time, detector ID and actuation duration length are stored. For signal events, signal start time, signal status, phase ID and signal duration length, are stored. The data sample and the format are shown in **Figure 3.6.**

Detector Actuation Event

Start Time of Detector "ON"	Detector ID	Duration length (Sec)
05:00:16.400	13	0.321
05:00:21.157	10	0.403
05:00:20.989	16	1.369
05:00:22.580	9	0.403

Signal Event

Start Time	Signal Status	Phase	Duration(Sec)
05:00:16.800	G	3	9.800
05:00:26.600	Y	3	4.000
05:00:33.100	G	4	10.300
05:00:43.400	Y	4	4.000

Figure 3.6 Data sample and format

Program Flow Chart of the Firmware

The flow chart of firmware for the DCUs is shown in **Figure 3.7**. When started, the DCUs first initialize the system clock, and attempt to establish the Ethernet connection with the remote data server. A watchdog timer is then enabled to automatically restart the DCUs if the program stops and idles for a long period. After Ethernet connection is established, the program will enter the main loop to enumerate input channels for on/off change. Each channel is associated with one detector or one signal phase. Once enough number of events, say, 10 events, are stored in the buffers, the data will be stored in log files and sent to central server.

Due to the different interfaces of the TS1 and TS2 DCUs, the firmware for the two is also different. The main difference is indicated in the red box in **Figure 3.7**. The TS1 DCUs check for voltage signal directly from the back panel pins, say, 24V for "detector on" and 0V for "detector off". For the TS2 cabinets, the signal status and detector status information is packaged within the SDLC frames transmitted through the SDLC bus (NEMA TS2 standard, 2002). Hence, instead of checking voltage signals, the TS2 DCUs check the associated data bits associated with detector and signal status from the SDLC frames, in order to identify change events.

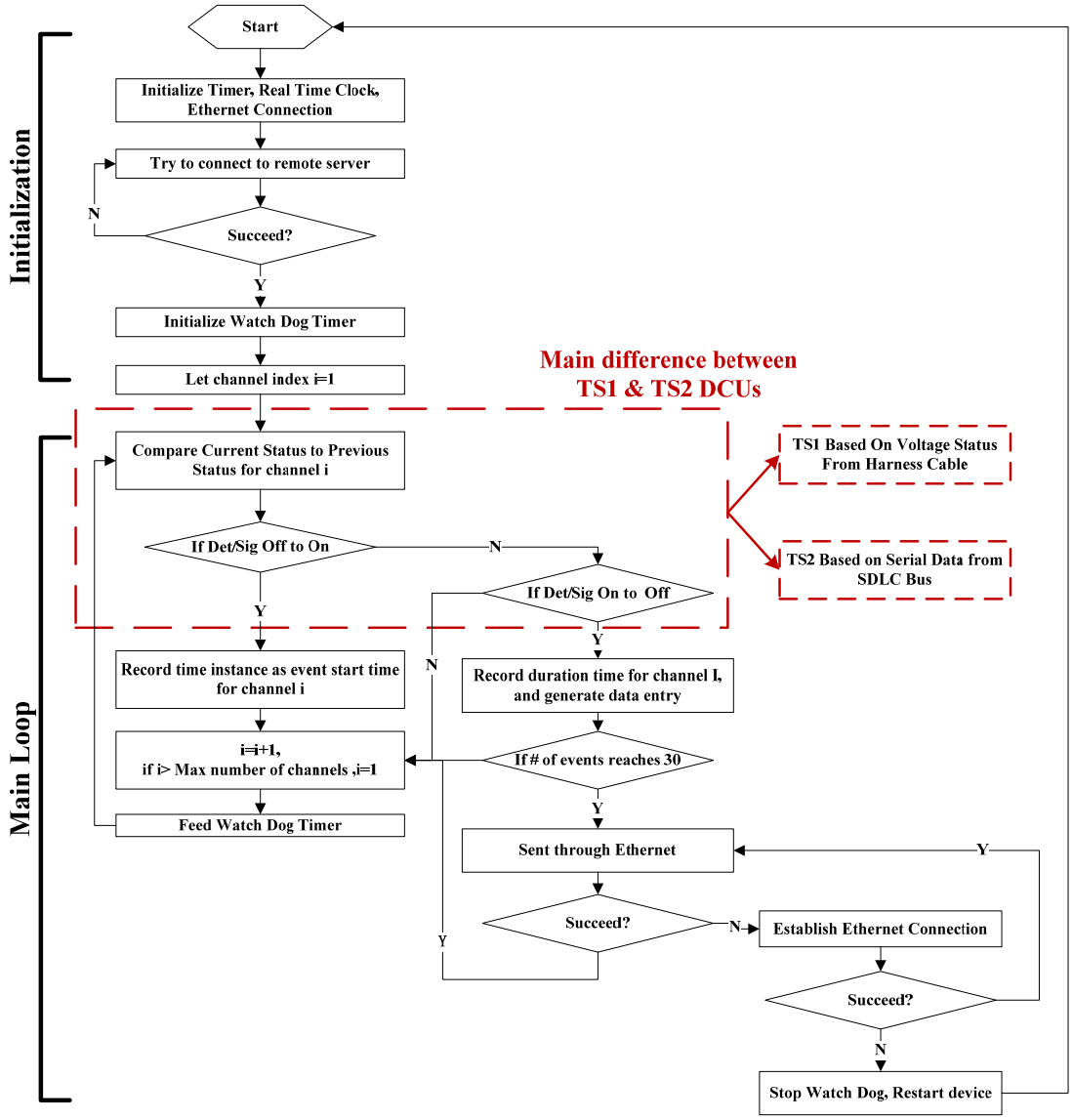

Figure 3.7 Flow chart of the firmware for the DCUs

Timing and Synchronization of DCUs

For the TS1 DCUs, a millisecond timer and a real time clock with 1 sec resolution are used, to time stamp the events. The clocks of the TS1 DCUs are synchronized with the central server via Ethernet, during midnight every day. For the TS2 DCUs, the time stamping mechanism is quite different. In the TS2 cabinet, the controller will broadcast its system time every sec, and signal status every 0.1 sec, to the SDLC bus. Every 0.1 sec, the detector bus interface units (BIUs) will transmit detector status with duration length of last detector actuation/de-actuation in millisecond resolution, to the SDLC bus.

Such mechanism is utilized in the TS2 DCUs. In details, the time stamping at 1 sec resolution of the TS2 DCUs is based on the controller broadcasting time. For signal events, the time stamping resolution beyond 1 sec remains at 0.1 sec, based on the time instant when signal frame data being transmitted by the controller. For the detector events, the time stamping resolution beyond 1 sec remains at one millisecond, based on the duration time from the BIUs. The synchronization of the data with central server is ensured automatically, as the controllers are synchronized with the central server in real time.

3.2.3 Installation and In-House Lab Testing

The installations of both DCUs are straightforward. For TS1 DCU, the procedures are:

1. Connect harness cable pin-to-pin to the contact closures on the back panel;
2. Plug in power adapter;
3. Connect the DCUs with Ethernet switch;
4. Turn on the power switch.

The procedures for TS2 DCUs are similar, except that the step 1 is to connect to SDLC interface instead of the contact closures. The procedures are illustrated in **Figure 3.8**.

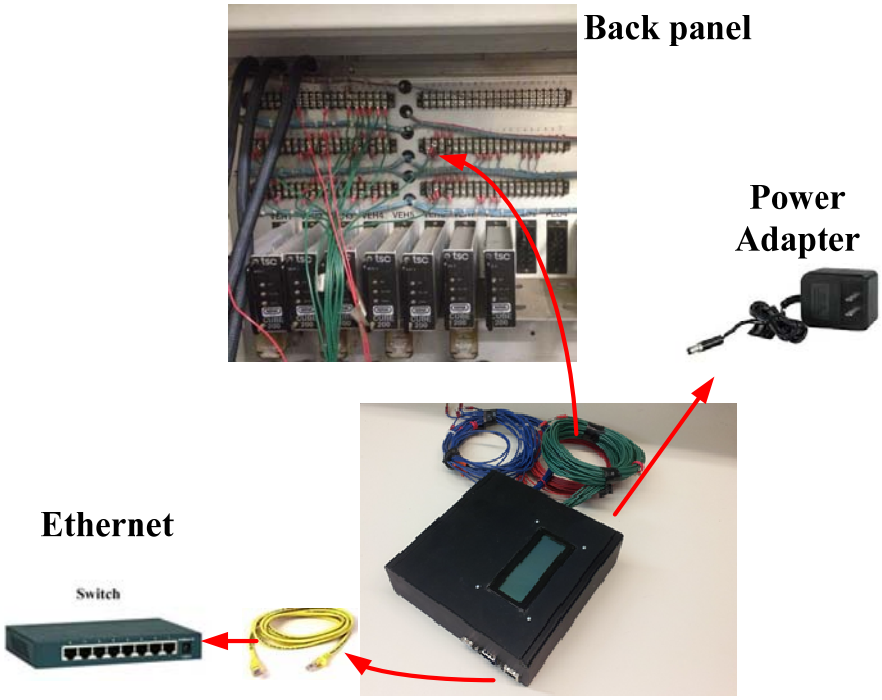

(A)

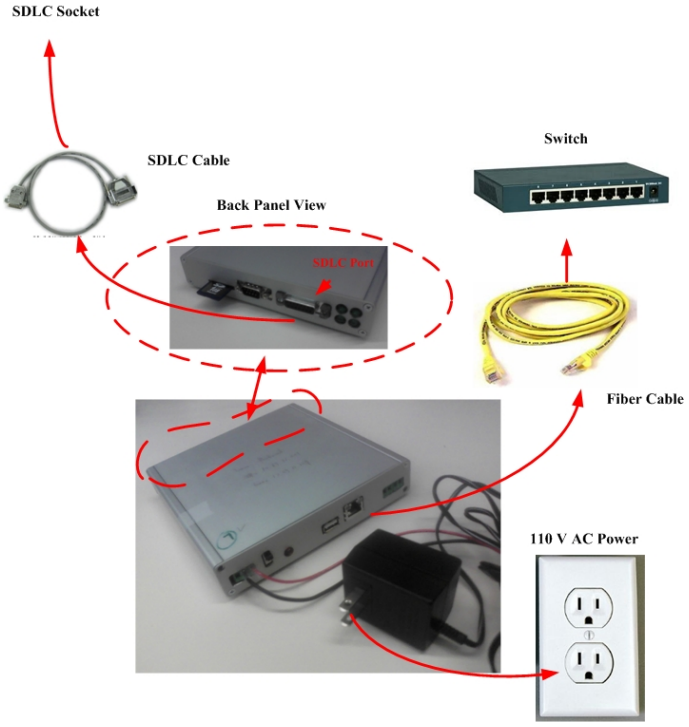

(B)

Figure 3.8 Installations of the TS1 DCU (A) and TS2 DCU (B)

Before deployments in the field, the DCUs were tested in the lab, using two

different platforms. The platform for TS1 cabinet is based on Hardware-In-the-Loop Simulation with VISSIM simulator, and the testing platform for TS2 is based on a commercial tester for TS2 controller, the TVC 3500 TS2 Virtual Cabinet by Athens Technical Specialists, INC. (ATSI). The snapshots and architectures of both platforms are shown in **Figure 3.9**.

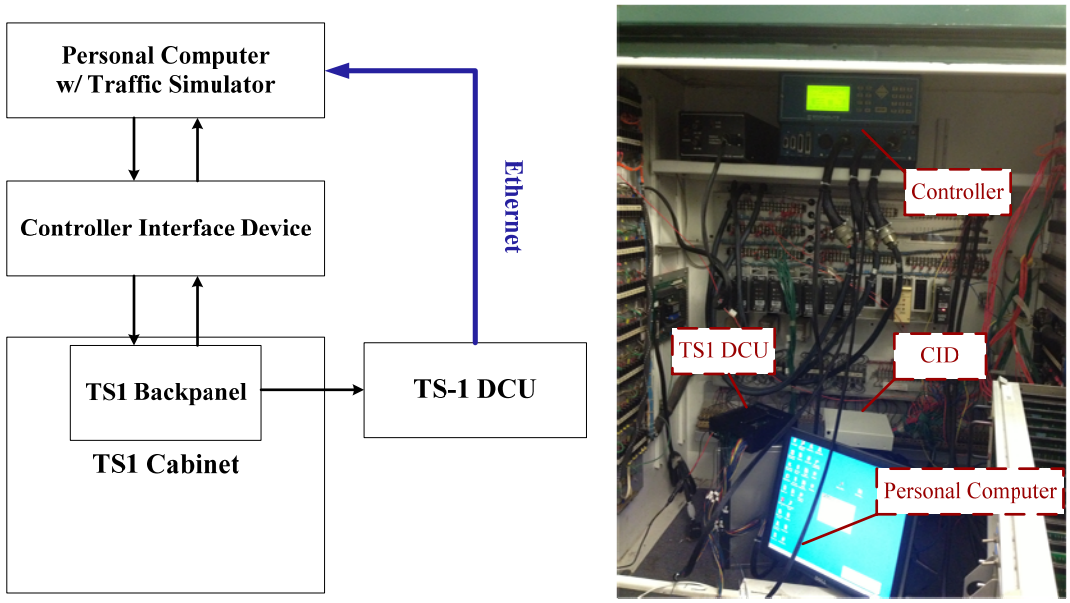

(A)

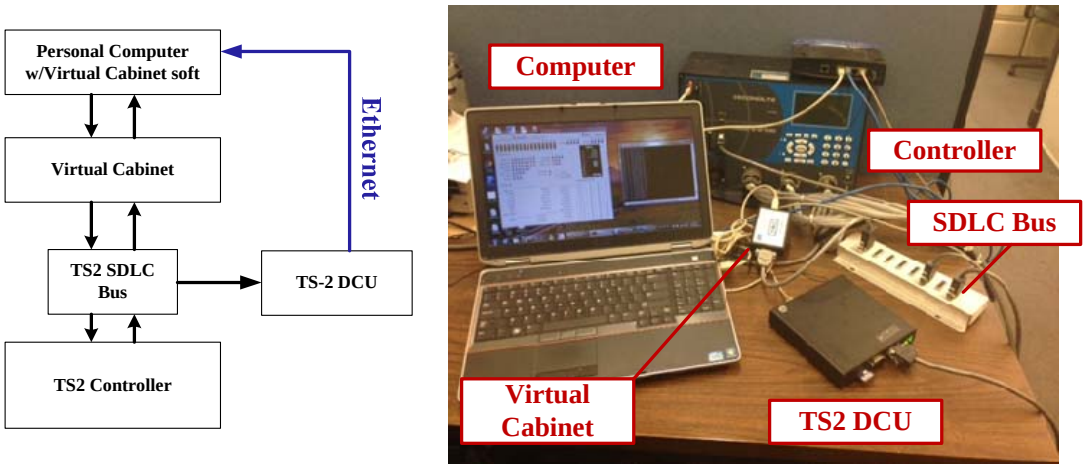

(B)

Figure 3.9 TS1 (A) and TS2 (B) Testing Platform

The testing platforms are aiming at simulating field intersections to test the performance of the DCUs. The vehicle detectors calls are generated by the software,

and sent to the controllers that run fully actuated signals. The DCUs will "listen to" and store changes of the detector status and signal status. At the same time, the simulated events information is stored separately in the computers for validation. Note that, in the TS1 testing platform, signal status is sent back to the simulation program to control traffic lights in the simulation program. Such feedback is not available for the TS2 testing platform due to the lack of application program interface (API).

Tests with 2-hour duration were conducted for both DCUs, resulting in 0% loss of data entries for TS1 DCUs, with a 2% average lost for TS2 DCUs. The data lost for TS2 DCUs could be mainly due to the additional computation load of TS2 DCUs to process SDLC frames. Nevertheless, 2% data loss should be in acceptable range in our applications for performance evaluation purpose.

3.2.4 Field Deployments

Since December 2011, TS2 DCUs have been installed at 12 intersections on Trunk Highway (TH) 13, Burnsville, Minnesota. These implementation sites are using fiber optics for communication between intersections and regional traffic management center (RTMC). A snapshot of DCU installed in field (Int. Lynn Ave & TH 13) is shown in **Figure 3.10**.

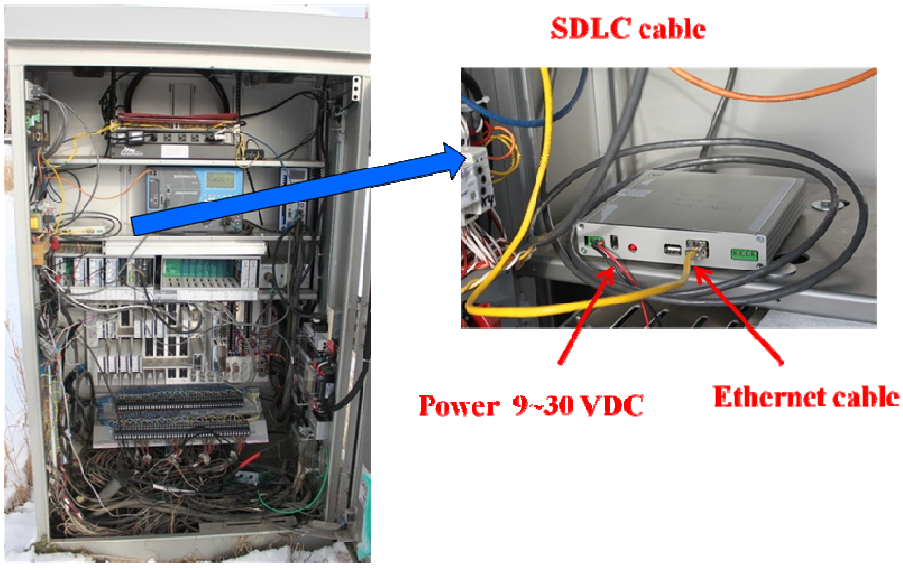

Figure 3.10 Snapshot of TS2 DCU installed at Int. Lynn Ave & TH 13

CHAPTER 4 OFFSET EVALUATION AND FINE-TUNING

This chapter will introduce the evaluation and fine-tuning module for the offsets, with focus on constructing TS-Diagram to visualize progression quality for arterials. The proposed procedure is demonstrated with field cases and validations were performed using detector data and probe vehicle trajectories data collected from fields. An experiment is then carried out to illustrate how signal parameter changes could be made by intuitively evaluating the generated TS-Diagram.

4.1 Background about Time Space Diagram

Time space diagram (TS-Diagram) is a popular visualization tool for traffic signal evaluation, and has been used widely for signal operations (Signal Timing Manual, 2008). With the time and distance as the X-Y axes, vehicle trajectories and signal status are commonly shown in a TS-Diagram. With the graphical illustration of the queues and delays, the progression quality can be evaluated intuitively. **Figure 4.1** plots one example of TS-Diagram, with trajectory of one vehicle and signal status at two intersections. Delay of the subject vehicle due to traffic signals can be clearly observed. If similar delays occur for the majority of the vehicles, a poor progression quality will be indicated.

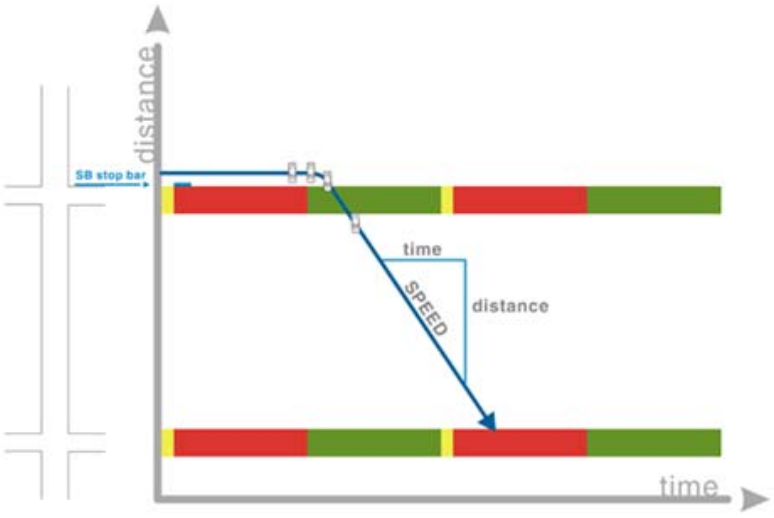

Figure 4.1 Example of TS-Diagram

[Source: Traffic Signal Timing Manual, 2008]

Because of such convenience, TS-Diagram has been utilized by several commercial software as an output of signal optimization. For instance, TRANSYT-7F plots TS-Diagram with the green bands, and Synchro provides options to plot simulated trajectories in its TS-Diagram (Wallace et al, 1998; Husch & Albeck, 2006). A screenshot of Synchro TS-Diagram is illustrated in **Figure 4.2**, with blue and red lines as the trajectories of southbound and northbound traffic, respectively.

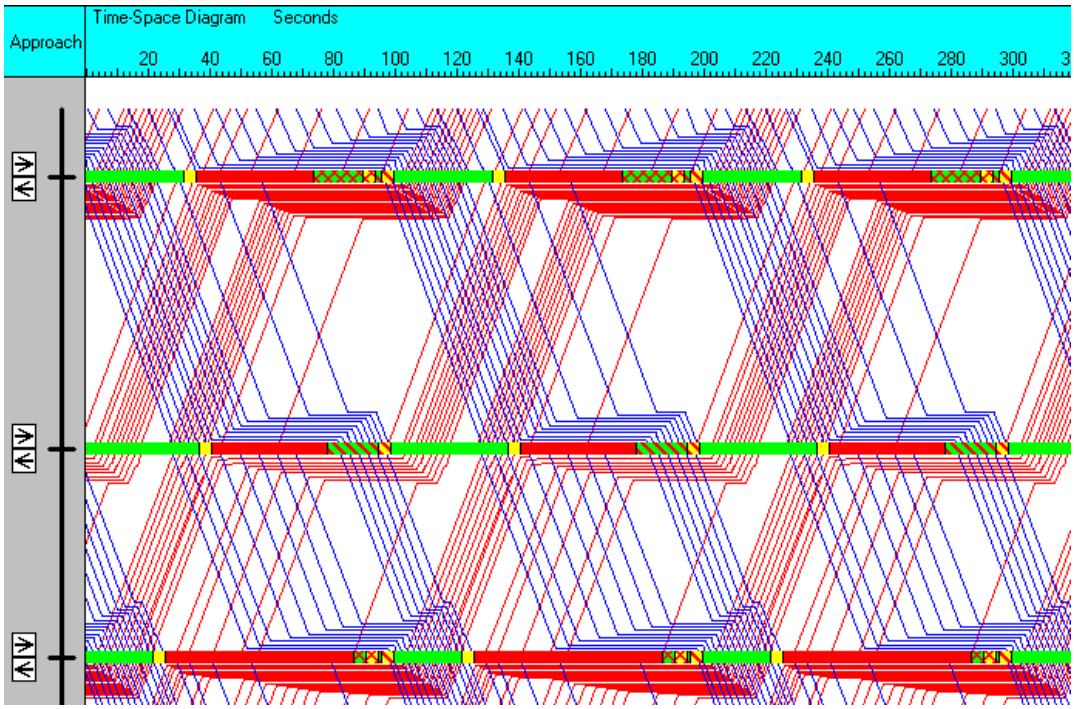

Figure 4.2 Screenshot of Synchro TS-Diagram

In the practice, the Synchro TS-Diagram is being used widely, to design or update signal timing parameters in the signal retiming process. An accurate Synchro TS-Diagram can properly reflect the field traffic condition, and help engineers choose appropriate timing parameters. On the contrary, inaccurate Synchro TS-Diagram, could mislead the engineers, degrade the timing performance, and increase the fine-tuning efforts. More importantly, since the Synchro TS-Diagram only uses manually collected data during a limited period, it cannot reflect the changing traffic conditions over time.

On the other hand, many intersections in the US are now using actuated signals, whereas few agencies have archived or analyzed the detector and signal status data to help signal operation (Liu et al., 2008). Recently, increasing attentions have been paid

on using detector and signal data for performance evaluation and optimization of the traffic signal system. However, to the best of our knowledge, few studies have been done to generate the TS-Diagram for evaluation of signal coordination. This research attempts to fill in this gap.

In this research, we propose a practical procedure to generate TS-Diagram using the high-resolution event-based traffic data collected from the field. With data collected and archived automatically, the TS-diagram can be generated periodically without significant labor cost. This is particularly beneficial for the practitioners to evaluate traffic signal performance after the retiming process, or to fine-tune the system over time. The proposed procedure is demonstrated with field examples and validations were performed using detector and probe vehicle trajectories data. Then, an experiment is demonstrated to illustrate how signal parameter changes could be made by intuitively evaluating the generated TS-Diagram.

4.2 Constructing Link TS-Diagram

The proposed procedure is to first generate TS-Diagrams for each link individually. Then, the link TS-Diagrams are combined as the arterial TS-Diagram. Note that, for two opposite through directions, there are two links between two adjacent intersections. The TS-Diagrams of these two links are overlapped, similarly to the Synchro TS-Diagram. Then the TS-Diagrams of consecutive links are stacked up sequentially, to form the arterial TS-Diagram.

In light of the cyclic nature of the traffic signal system (Day et al., 2010), the TS-Diagram is constructed cyclically using data aggregated from multiple cycles. This indicates no variations of traffic patterns over different cycles in the plot. The reason is that traffic signal parameters are generally governed by dominant cyclical patterns while variations from cycle to cycle are usually limited with TOD operation. Moreover, the aggregation can help reduce the data noise from the detector, and make it easy to evaluate the average performance of a timing plan. Two steps are involved to generate a link TS-Diagram, described as follows.

Step 1. Aggregating high-resolution event-based data

In this step, both detector and signal data are aggregated. The detector event data is aggregated as the average cyclic flow profile (CFP), i.e. the interval volume over time within a cycle. Note that, the CFP has been used in TRANSYT-7F and SCOOT system (Wallace et al., 1998; Robertson & Bretherton, 1991), as well as some other researches for offset optimization (Abbas et al., 2001;Gettman et al., 2007; Day & Bullock, 2011). Here, we calculate the CFP of the through traffic at the link entrance, based on the advance detector data. To do so, the time instances of vehicle arrivals at the link entrance are estimated first. Depending on the queue impacts on the detector data, two cases need to be considered.

Case A: Queue does not propagate to the advance detectors

In this case, all vehicles would travel from the entrance to detector location in free flow speed. Hence, the arrival time at entrance are estimated by simply shifting the arrival time at the detector location with free flow travel time, as expressed by formula (4.1).

$$t_e(k) = t_d(k) - \frac{l_d}{v_f} \quad (4.1)$$

Where:

$t_e(k)$ is arrival time of k th detector actuation event at link entrance,

$t_d(k)$ is start time of k th detector actuation event at detector location and is measured directly,

l_d is distance from detector location to the link entrance, and

v_f is free flow speed.

Case B: Queue propagates to the advance detectors

In this case, vehicles may not all travel freely from the entrance to detector location, as some vehicles are delayed by the queue. Hence, the shifting in formula (4.1) is not applicable for all arrivals. Such cases can be identified with the queue over detector (QOD) phenomena from the detector data (Liu et al, 2009; Wu et al., 2010). This is illustrated in **Figure 4.3**. After the red starts, if a long queue exists, the detector will see vehicles standing at the detector location for unusually long time. The end time of this particular actuation event is when the vehicle on the detector starts to move after green

starts, followed by queuing vehicles passing the detector at a saturated departure rate. In **Figure 4.3**, Point A indicates the time when queue propagates to the detector location. Point B indicates the time when the queuing vehicle on the detector starts to move, and Point C indicates the time when the last queuing vehicle passes the detector. The arrivals between points A and C are delayed by the queue, and need further adjustment to estimate their arrival times at the entrance. The corresponding detector status is also shown in **Figure 4.3**.

To estimate the arrival time of the delayed vehicles, we adopt the algorithm in (Liu et al., 2009). Essentially, the algorithm attempts to identify three points A, B, and C based on the occupancy times and the time gaps from the vehicle-detector actuation event data. The points A and B can be identified as the start and the end of a detector event with long duration time. Point C, the end of queue departure, could be identified as the end of consecutive saturated departure events after green start, followed by a large gap. For more details of identifying point A, B, and C, we refer to (Liu et al., 2009). After the points A, B, C are identified, the arrivals are assumed as uniform arrivals between Point A and C, as expressed in the formula (4.2).

$$t_e(k) = \begin{cases} t_d(k_A) + \dfrac{(k-k_A)}{k_C - k_A}[t_d(k_C) - t_d(k_A)] - \dfrac{l_d}{v_f}, for\ k \in [k_A, k_C] \\ t_d(k) - \dfrac{l_d}{v_f}, Otherwise \end{cases} \quad (4.2)$$

Where:

k_A is index of detector event starts at Point A, and
k_C is index of detector event at Point C.

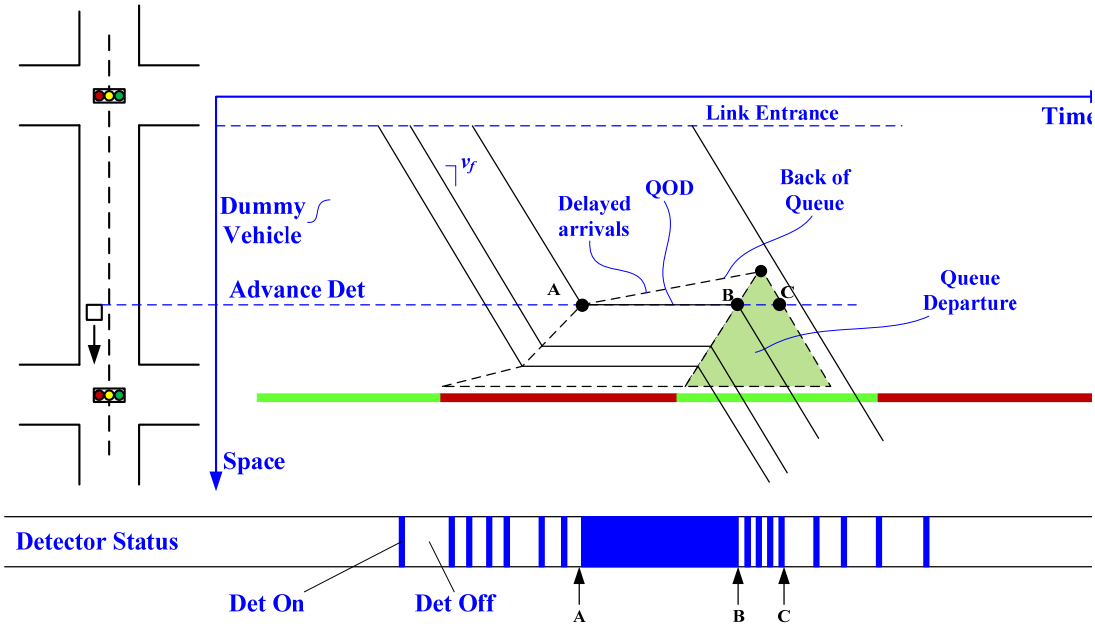

Figure 4.3 Illustration of queuing at intersection with QOD

Based on the estimated arrival times at the entrance, the interval volume can be then calculated using formula (4.3).

$$q(j) = \sum_{k=1}^{N} \mathbb{1}\{j\Delta t \le t_e(k) < (j+1)\Delta t\}, \qquad for\ j = 1,2 \dots T. \quad (4.3)$$

Where:

$q(j)$ is volume of j th interval over investigation period,

Δt is the length of interval,

j is the index of interval over investigation period,

N is the total number of detector events,

T is the total length of investigation period, normalized by Δt, and

$\mathbb{1}\{.\}$ is the indicator function, with 1 if condition within bracket is satisfied, and 0 otherwise:

Then, the average CFP can be obtained by aggregating interval volume over cycles using formula (4.4). One example of the CFP with 5 sec interval is shown **Figure 4.4.**

$$\hat{q}(i) = \frac{\sum_{Mod(j,C)=i} q(j)}{N_c}, \qquad for\ i = 1, \dots, C. \quad (4.4)$$

Where:

$\hat{q}(i)$ is flow of i th interval over time within cycle, as the CFP,

N_c is total number of cycles during investigation period,

C is for cycle length, which is the cycle length divided by Δt, and

Mod (,) is the modulo operator.

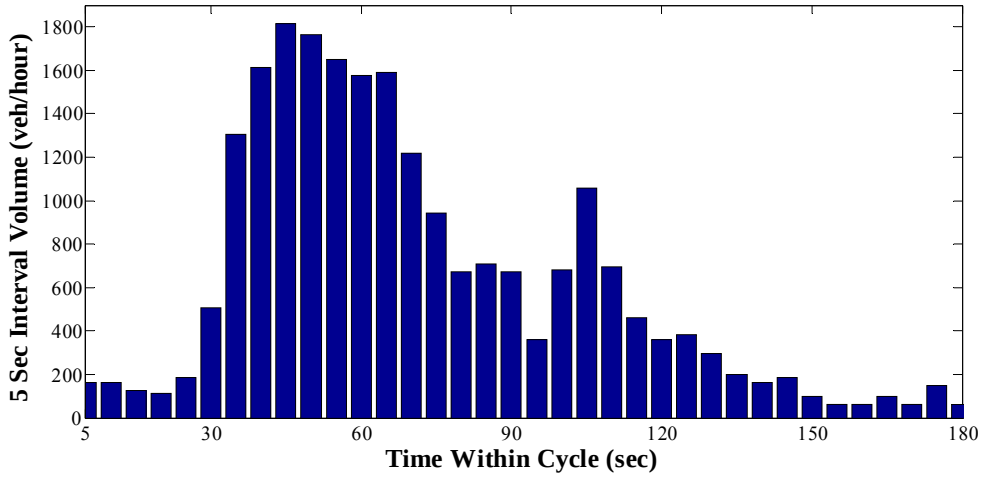

Figure 4.4 Example of CFP

Based on signal event data, the average green start and end of the associated phase are calculated by formula (4.5). For simplicity, yellow signal is treated as part of red signal.

$$\begin{cases} \bar{t}_{gSt} = \dfrac{\sum_{k=0}^{N_c} Mod(t_{gSt}(k), C)}{N_c} \\ \bar{t}_{gEd} = \dfrac{\sum_{k=0}^{N_c} Mod(t_{gEd}(k), C)}{N_c} \end{cases} \quad (4.5)$$

Where:

$\bar{t}_{gSt}$ is the average green start time over time of cycle,

$t_{gSt}(k)$ is the time of k th green start,

$\bar{t}_{gEd}$ is the average green end time over time of cycle,

$t_{gEd}(k)$ is time of k th green end, and

all variables including $\bar{t}_{gSt}$, $t_{gSt}(k)$, $\bar{t}_{gEd}$, $t_{gEd}(k)$ are normalized by Δt.

Step 2. Generating Virtual Trajectories

The CFP, average green start and end will be used to generate the link TS-Diagram. Before plotting, based on the CFP, a sequence of time instances at the link entrance will be generated, simulating virtual vehicles entering the link. This is a little tricky, due to the non-integer flow rate during an interval. For instance, with a 5 sec interval length, if a 1800 vehicle per hour (vph) flow rate is observed for the 1st interval, and 800 vph for the 2nd interval, , the problem is then to simulate 2.5 vehicles during 1st interval window, and 1.25 vehicles for the 2nd interval. One approach is to rounding up the numbers of vehicles, but it will introduce substantial rounding up errors. Instead, we simulate 250 vehicles equally spaced in the 1st interval, and 125 vehicles in the 2nd interval. Then, 100th, 200th, and 300th vehicles over the 10 sec horizon will be selected as the virtual arrivals to generate the trajectories. This approach can be viewed as generating fraction of vehicle based on flow rate. Then fractions are accumulated as whole vehicles.

At each time instance, a vehicle is simulated traversing from the entrance to stop bar, using the Newell's simplified car following model (Newell, 2002). In Newell's model, the follower's trajectory is simply a temporal-spatial translation of the leader in car-following mode. The calculation is expressed in formula (4.6).

$$x_i(t+\tau) = Min\{x_{i-1}(t) - d, x_i(t) + \tau v_f\} \quad (4.6)$$

Where:

$x_{i-1}(t), x_i(t)$ are the trajectories of the leader and follower respectively,

τ is the time displacement, and

d is the space displacement.

To account for the signal impact, a dummy vehicle based on red signal is generated as the first leading vehicle within the cycle. The procedure is repeated cycle by cycle to expand the plot. The illustration of the dummy vehicle is shown in **Figure 4.5.**

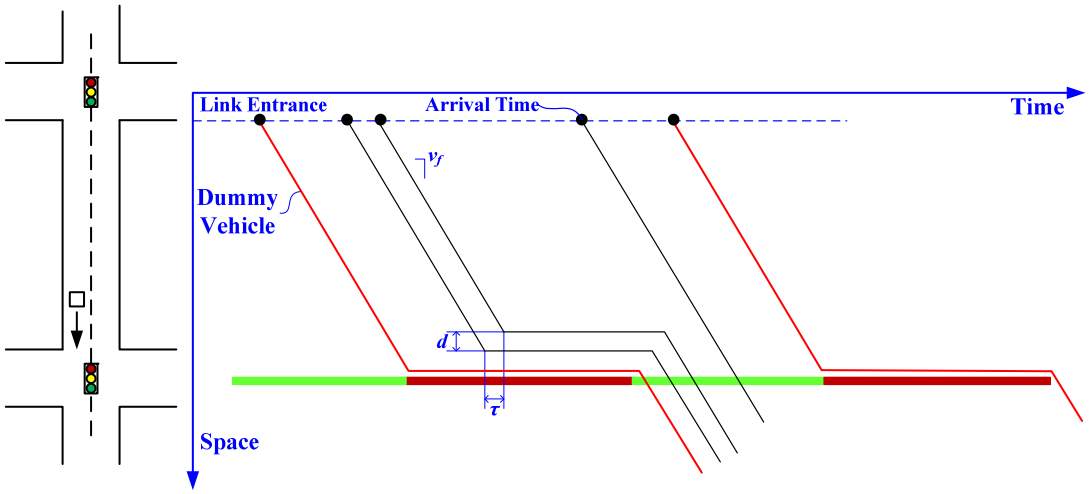

Figure 4.5 Illustration of car following and dummy vehicle.

4.3 Validation of TS-Diagram

Two cases are demonstrated, using data collected on Trunk Highway (TH) 55 and TH 13 in Minnesota. Both arterials are operated with vehicle-actuated coordinated control. Here, the parameters of the car following model are not calibrated but using typical values. In details, the post speed limit was used as the free flow speed, around 50 mph. 30 ft and 1.6 sec were used for the space and time displacement, approximately leading to jam density of 175 vehicle per mile (vpm) and capacity of 1800 vph.

4.3.1 Case 1: TH 55

Five intersections on TH 55 deployed with the SMART-Signal system are highlighted, with data collected on Nov 17th, 2008, from 7:15 AM-8:45 AM, when the morning peak timing plan was running. The TS-Diagram are shown in **Figure 4.6**, with arterial layout. In addition to the advance detectors, there were also temporary detectors at the link entrances for research purpose. The eastbound (EB) and westbound (WB) trajectories are plotted with blue and red lines, respectively. The associated signal status for each direction was plotted facing the corresponding trajectories. As can be seen clearly, although the link TS-Diagrams were constructed independently, the traffic patterns were consistent across intersections, reflecting the consistent progression impact from the signal. This can also be viewed as a preliminary validation of traffic patterns in the TS-Diagram.

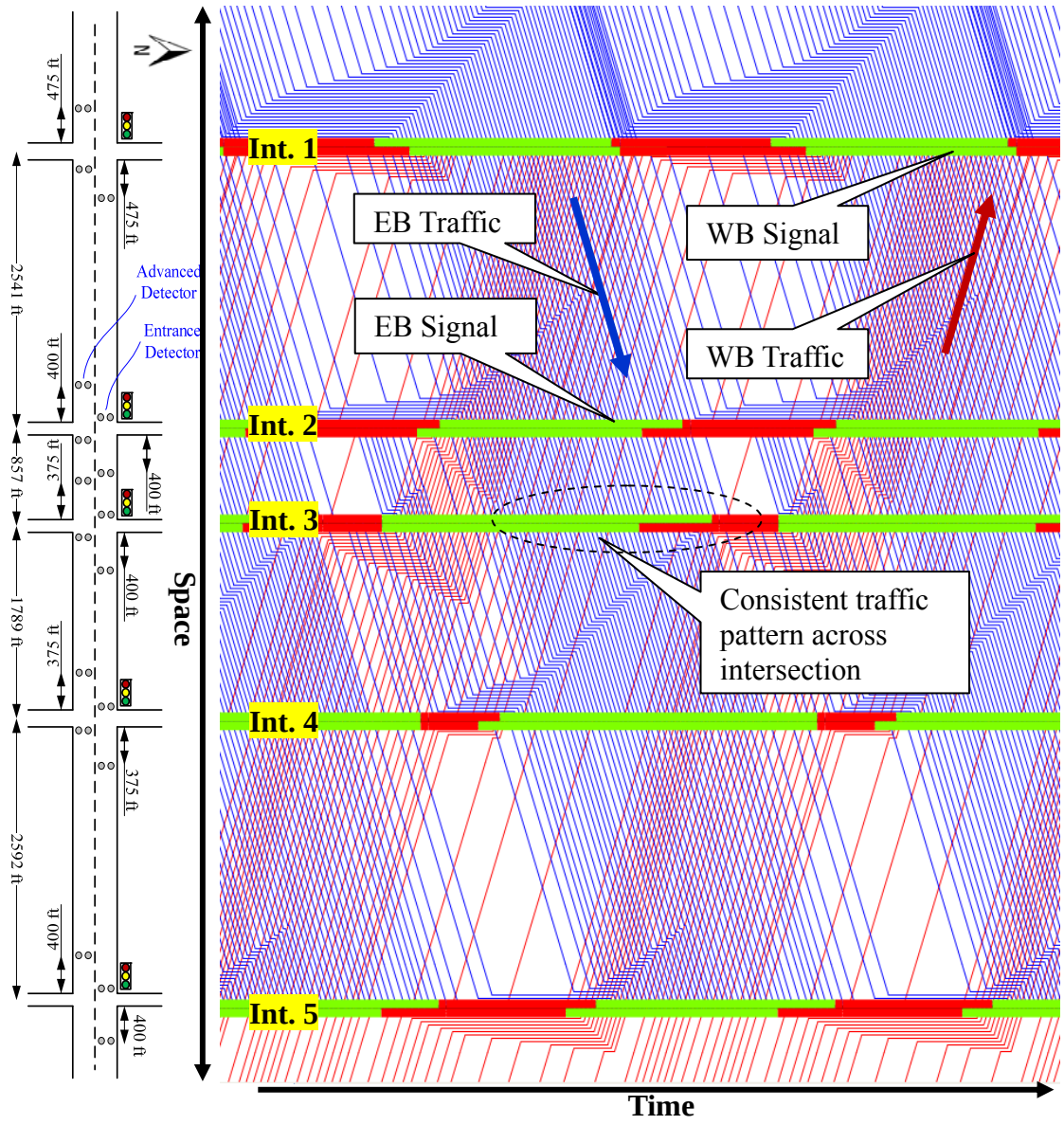

Figure 4.6 Layout and TS-Diagram for TH 55

Using data from the entrance detectors, a comparison was conducted, regarding the estimated and observed CFPs at the entrances. For each link, the total volumes from advance detectors and entrance detectors were balanced to reduce the impacts from the sinks and sources. The result is shown in **Figure 4.7**. As we can see, the estimated CFPs match well with the observed CFPs, indicating good estimation by the proposed method.

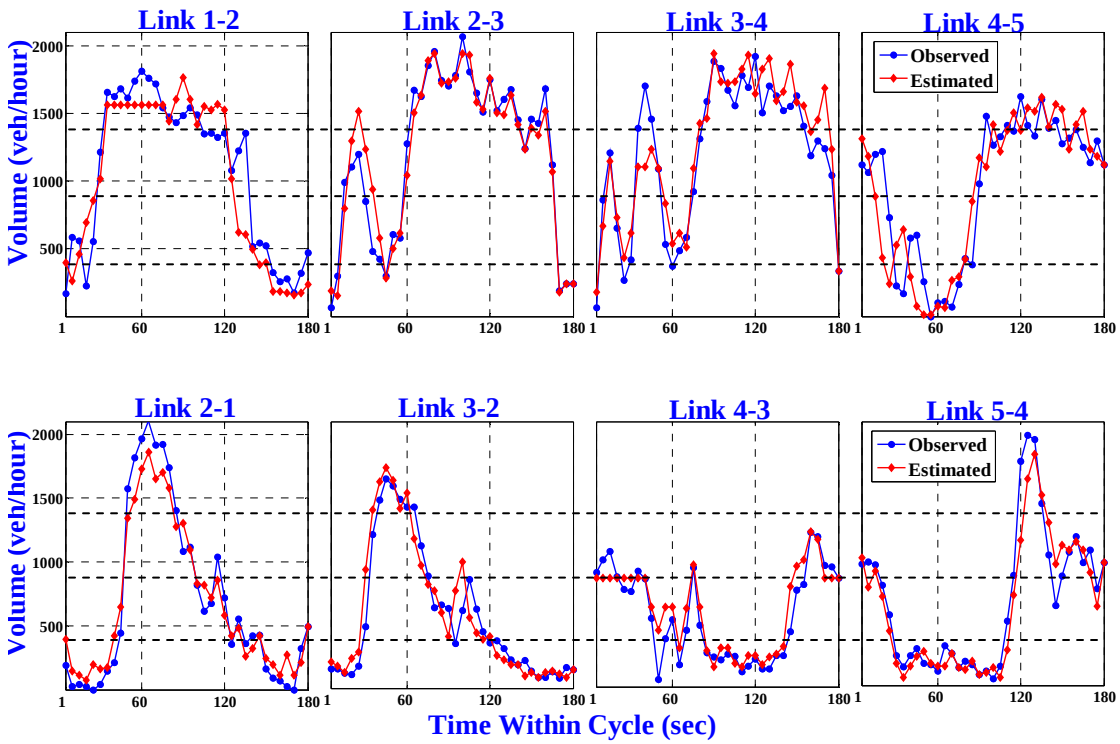

Figure 4.7 Estimated CFPs VS Observed CFPs for EB(Up) and WB (Down) traffic

4.3.2 Case 2: TH 13

In this case, seven intersections on TH13 with the SMART-Signal system were selected. The data was collected during afternoon peak period, from 4:30 to 6:00 PM, on Jul 23, 2013, with GPS data of nine field rides through the selected intersections. The TS-Diagram is shown in **Figure 4.8**, with the field ride trajectories in black. Note that, the field rides were actually made during several cycles, but were plotted within a single cycle based on individual departure time within each cycle at both ends of the arterial.

As indicated in the figure, the EB trajectories match well with the generated TS-Diagram, while some disagreements were found, indicated by letter A and B. This is expected as the TS-Diagram only reflects the average conditions, and cannot reflect the variations of the green start due to side street actuations and pedestrian calls. Similar disagreement was found for WB trajectories at Int. 6, denoted by C. However, significant disagreements were observed for WB trajectories approaching Int. 5, denoted by D. This was mainly due to the occurrence of WB oversaturation and residual queues at Int. 5. Due to the residual queues, the repetitive patterns were interrupted,

resulting in amplified variations over cycles. This is evident from the significantly different trajectories traversing the intersection, while the vehicle entered the link at similar times within cycle. This indicates a limitation of the proposed TS-Diagram for the oversaturated intersections.

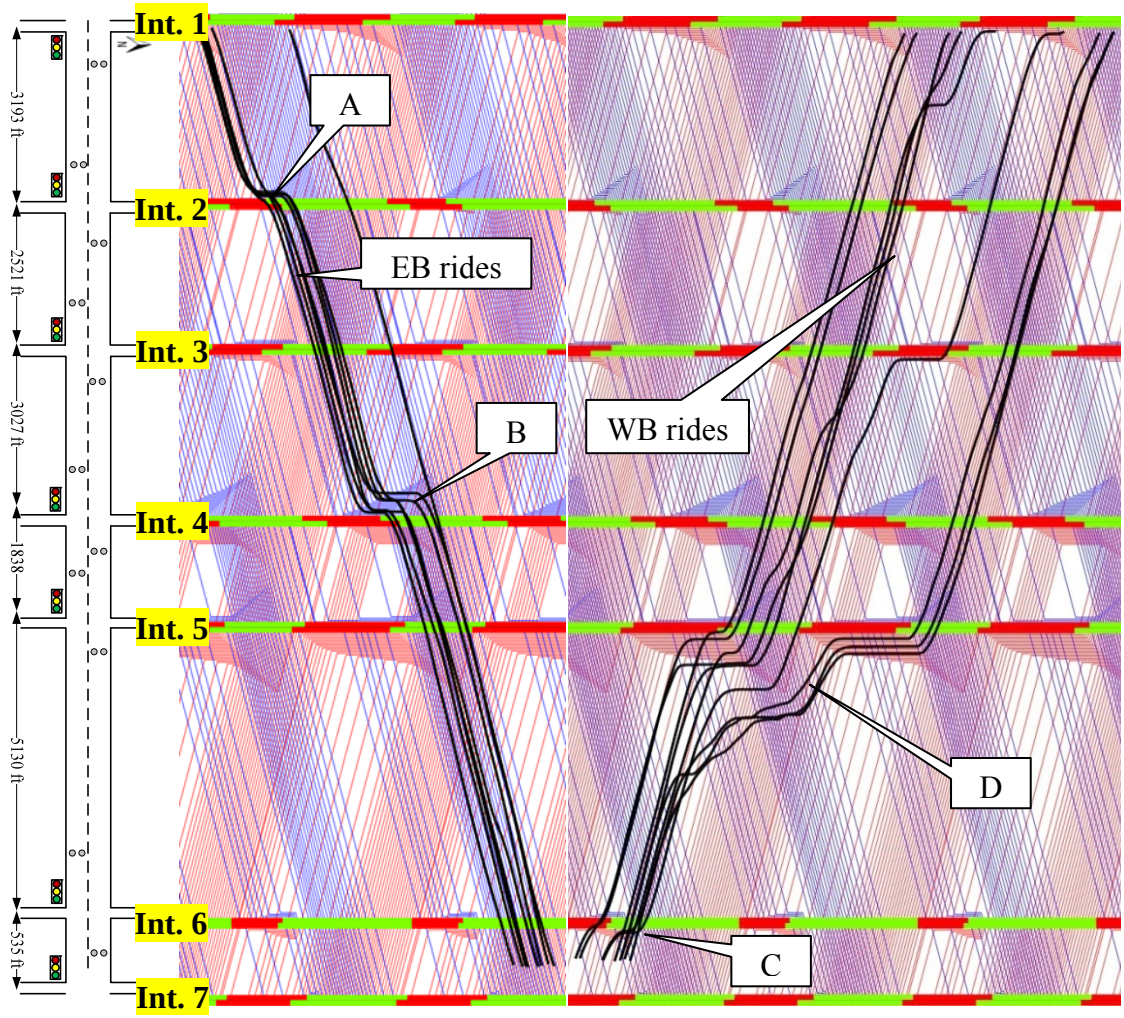

Figure 4.8 TS-Diagrams for selected intersections on TH 13

4.4 Fine-Tuning Using Ts-Diagram with Offset and Lead-Lag Sequence

To illustrate the potential application of the TS-Diagram, an experiment was carried out to adjust the offsets and main street phase sequence, i.e. the lead-lag sequence, indicating whether the main street left turn phase is leading or lagging the through phase, for a eight-phase dual-ring NEMA controller. For the offset, we use green start of first coordinated phase as the reference point. Regarding the lead-lag sequence, there are

four possible configurations for an eight-phase dual-ring NEMA controller, as shown in **Figure 4.9**. The configuration can be identified easily from the shape of overlapping green signals in the TS-Diagram.

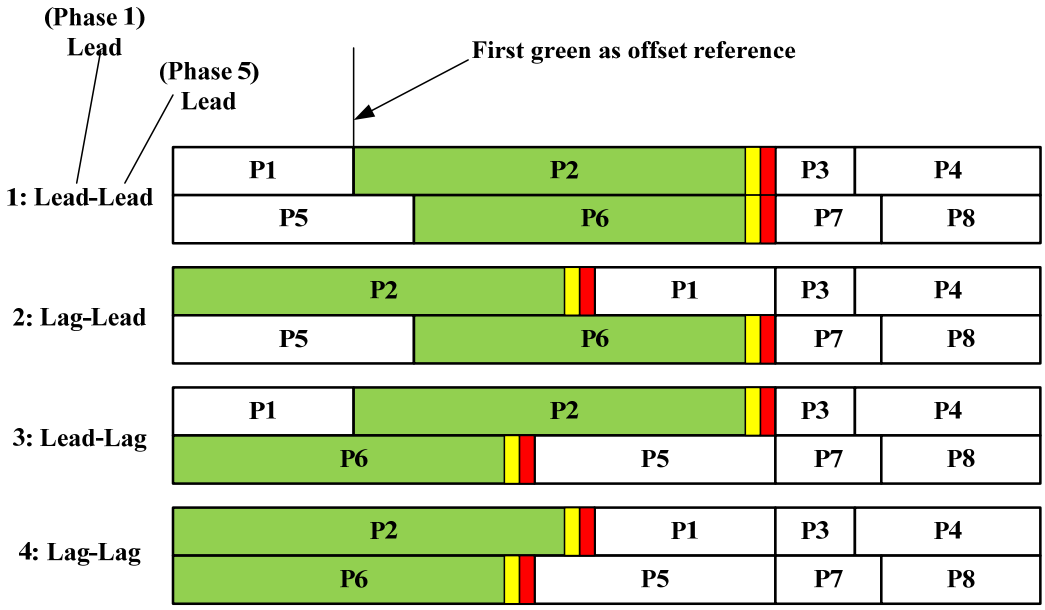

Figure 4.9 Offset reference point and combinations of lead lag sequence

So far, the TS-Diagrams are generated based on average data, reflecting the average traffic conditions. Many agencies, however, may concern about traffic signal performance for congested traffic conditions. To address such concerns, we also construct the TS-Diagram for relatively congested conditions, which will be the base of the analysis hereafter. To do so, when aggregating the raw data, the cycle volumes are calculated and ranked. Then, cycles with high cycle volume is kept and the rest will be filtered out. Here, we kept data with the highest 60-100 percentiles cycle volumes for each intersection, and constructed the TS-Diagram for the congested conditions. In practice, the criteria can be user specified, while our choice of 60-100 percentiles is to reflect relatively congested yet not extreme cases.

Both of the TS-Diagrams are shown in **Figure 4.10**, with Int.1 to Int. 5 of TH13 highlighted for analysis. The data was collected on four consecutive weekdays, 10/28/2013 to 10/31/2013, during 7:15 to 8:45 AM, for the evaluation of morning peak timing plan. Note that, while main traffic patterns remained similar, the queues were

clearly longer in the congested case than the average case, indicated by letter A and B.

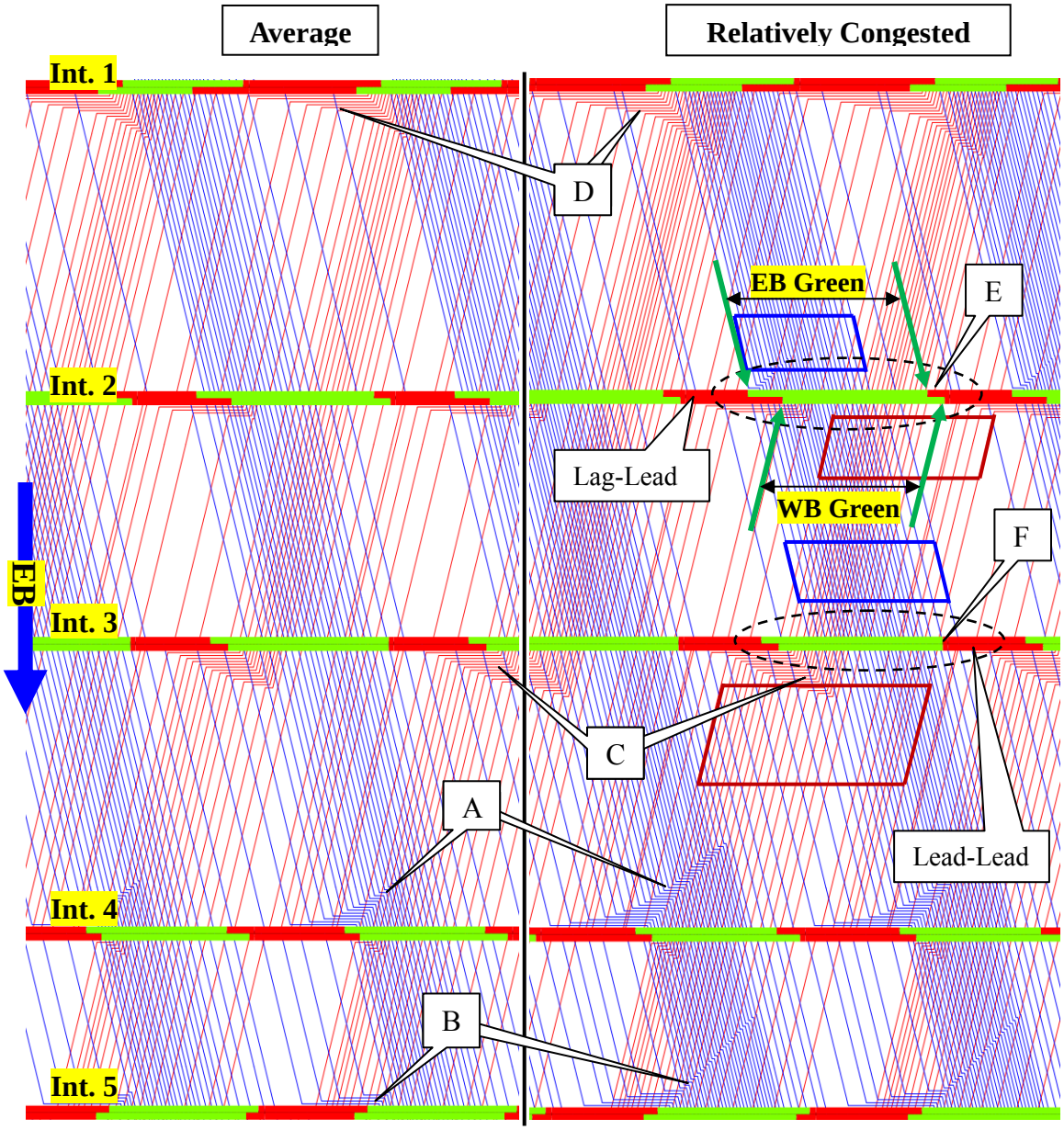

Figure 4.10 TS-Diagrams for selected intersections on TH 13 with average (left) and relatively congested conditions (right)

For a two-way coordinated arterial, trade-off exists for traffic in the opposite directions. With TS-Diagram, established method e.g. MAXBAND or combination method (Little, 1966; Gartner & Little, 1973; Day & Bullock, 2011) can be incorporated easily. could be incorporated for optimization. Here, instead of using a specific optimization method, we performed a quick, visual based evaluation of the TS-Diagram

for the changes. Indeed, this would involve engineering judgment, and may lead to sub-optimal solution. For the sake of illustration, we will the visualization approach with this analysis, leaving systematic optimization for future research.

First, the queue length and delays were identified from the TS-Diagram. In **Figure 4.10**, the EB cases are indicated by letter A and B, with the WB cases by C and D. The offsets were first fine-tuned for the direction with larger volume. The opposite direction was optimized next. Here, the EB was favored with a higher volume. The queues indicated by A and B, in the congested case, could be reduced by slightly shifting offsets to the left. The tradeoff exists with degraded WB performance at Int. 3 and Int. 4. This, however, should be minimal with the lower volumes. The decision was made to shift the offset at Int. 4 to the left for 4 sec, and 4 sec further to the left for offset at Int. 5, with a total 8 sec to the left at Int. 5. The 4 sec was selected arbitrarily because we want implement small adjustments only.

For the WB cases, to reduce the queue labeled with C, either the offset at Int. 3 needs to be shifted to the left, or offsets at Int. 4 and Int. 5 to the right. If offset at Int. 3 were shifted to the left, the end of EB platoon at Int.3 would be cut off and delayed by the red. If offsets at Int.4 and Int.5 were shifted to the right, the EB queues and delays would increase at Int. 4. Considering queue labeled with D, the end of the WB platoon was close to the green end, and would be delayed if offset were shifted to the left. Considering the overall benefit, no offset changes were justified regarding the WB cases.

Next, lead-lag sequences were evaluated. Here, we search for configuration of the lead-lag sequences that provides the max green window for the platoons in both directions. One example of a proper lead-lag sequence is indicated by E. The overlapping shape of platoon arrivals (EB first), indicated by the blue and red parallelograms was consistent with the overlapping shape of the green windows (EB first) for the two directions. This indicates the current setting of Lag (phase 1)-Lead (phase 5) was appropriate at Int.2. The intersections were evaluated one by one with similar logic. One potential change was identified, indicated by F. In this case, the end of EB platoon was cut off by the red signal, and could be better served by changing the Lead-Lead to Lead-Lag. The change was then granted. In addition, to accommodate the

lead-lag change, the offset in Int. 3 was also shifted 7 sec to the left, so that there would not be unused EB green time after the end of EB platoon.

The offset and lead-lag changes are summarized in left part of **Figure 4.11**. For better illustration, the shifts of individual phases are indicated by the arrows. The changes were implemented from 11/05/2013 to 11/07/2013. Due to a connection issue, the data for 11/06/2013 was not available. The TS-Diagram generated using data collected on 11/05/2013 and 11/07/2013 is shown on the right part of **Figure 4.11**.

Slight changes of traffic patterns were found from **Figure 4.11**. For EB traffic, the shockwave at Int. 2, indicated by A, was slightly reduced. The EB arrivals near the start of red at Int.3 was better accommodated, indicated by B. No obvious change was found for the EB arrivals at Int.4, indicated by C. This is intriguing given the relatively large shift of EB phase at Int. 3. If observed carefully, the density of the lines for the arrivals has changed slightly as circled by the blue parallelograms, and both arrivals showed slight inconsistency with departures at Int. 3. The potential interpretation is as follows: in the before case, the drivers decelerated with anticipation of the queue formation, and the queuing profile at Int. 4 were based on the delayed arrival time, and were underestimated. For WB traffic, degraded performance was found at Int.1, Int.3 and Int.4. Some improvements were found at Int. 2, labeled by E, likely because main street arrivals near the green start and arrivals from the site street at Int. 3 were better coordinated.

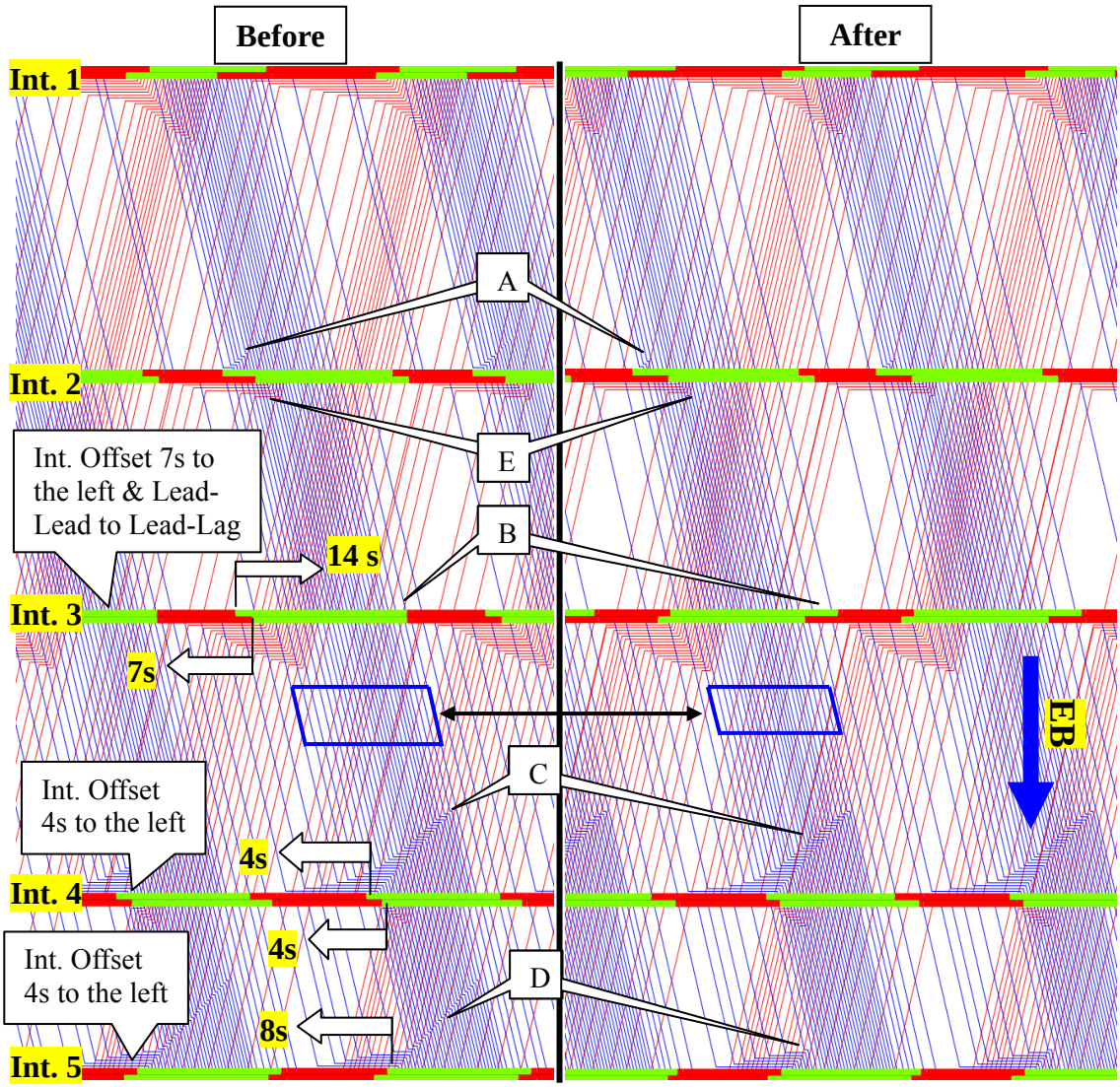

Figure 4.11 Before-After comparisons of TS-Diagrams with relatively congested condition

For further validation, the queue length and delay were estimated by the SMART-Signal system (Liu & Ma, 2009; Liu et al, 2009; Wu et al, 2010), and the results are summarized in **Figure 4.12** and **Table 4.1**. As indicated in **Figure 4.12**, average maximum queues were reduced for most of EB phases, while slightly increased for the WB phases. This is consistent with the TS-Diagram, as the proposed changes favored EB over WB traffic.

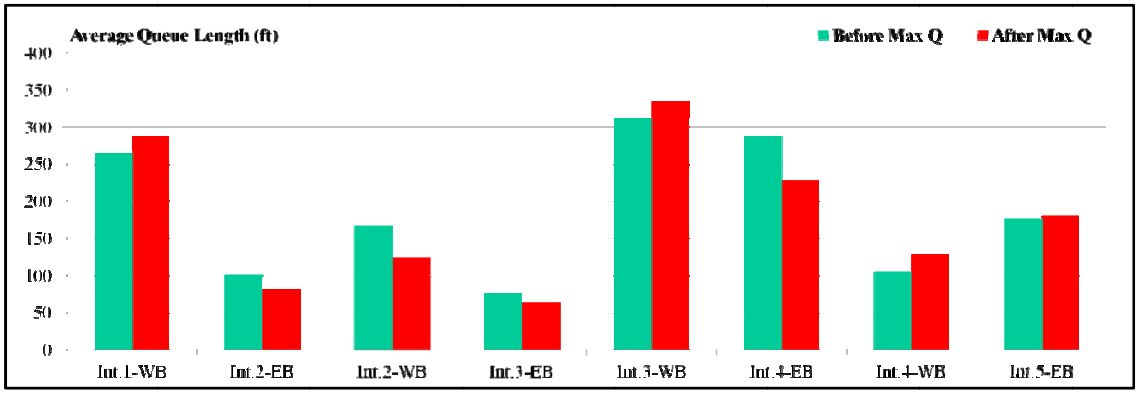

Figure 4.12 Before-After comparison of maximum queue length from SMART-Signal System

As indicated in **Table 4.1**, the average delay for EB travel was reduced by 14%, with 4.6 sec/veh, while for WB traffic, it increased by 4%, with 2.7 sec/veh. Overall, with the higher volume of EB traffic, the total delay was reduced by 4%, i.e., 163.8 veh sec/cycle.

Table 4.1 Before-After comparison of delay from SMART-Signal System

Average	Before	After	Abs. Change	Per. Change
EB Vol. (vph)	1314	1310	-4	0%
EB Delay (sec)	32.4	27.8	-4.6	-14%
WB Vol. (vph)	1003	1007	4	0%
WB Delay (sec)	65.3	68	2.7	4%
Cycle Delay (Veh*Sec)	4607.6	4443.8	-163.8	-4%

CHAPTER 5 GREEN SPLITS EVALUATION AND FINE-TUNING

This chapter will introduce the performance evaluation and fine-tuning module for the green splits.

5.1 Measure of Effectiveness for Green Splits

Assigning green splits proportionally to traffic demands is a simple while effective rule to determine green splits. To evaluate the performance of green splits, classical measures of effectiveness (MOE), volume/capacity ratio (v/c ratio), is commonly used when designing signal timing parameters. However, in the conventional practice, the v/c ratios are only calculated during signal retiming process with manual collected data, and are not monitored continuously. Although the practice is limited, there are some researches trying to calculate v/c ratios using the detector and signal data for evaluation of the green split and cycle length (Balke & Herrick, 2004; Balke et al., 2005; Smaglig et al., 2007; Day et al., 2010; Sunkari et al., 2011).

The green splits fine-tuning module proposed here can be viewed as an extension from (Smaglig et al., 2007; Day et al., 2010). The main difference is, instead of using detector volume directly, we proposed a new MOE, the Utilized Green Time (UGT), extended from the queue service time (QST) for green split evaluation. The purpose is to address the issue that volume measured at stop bar detectors could be inaccurate, since the stop bar detectors are mainly for vehicle presence detection, especially when long or sequential detectors are used (Lawrence et al., 2006).

5.1.1 v/c ratio

The v/c ratio indicates saturation level of a specified signal phase (Highway Capacity Manual, 2000), and can be calculated cycle-by-cycle, as:

$$X_i(j) = \frac{V_i(j)}{s_i x_i(j)} \qquad (5.1)$$

Where:

$X_i(j)$ is the v/c ratio of phase i, for j th cycle,

$V_i(j)$ is the flow rate of phase i, for j th cycle,

s_i is saturation flow rate of phase i,

$x_i(j) = \frac{g_i(j)}{c}$ is the green split, and,

$g_i(j)$ is the green time.

When long or sequential detectors are used, vehicle counts could be inaccurate. This is because consecutive arrivals may only cause a single detector actuation event with long duration length. One example from a sequentially connected detector at stop bar is shown in **Figure 5.1**, with example of detector actuation events. In such cases, occupancy-based measures will be more desirable.

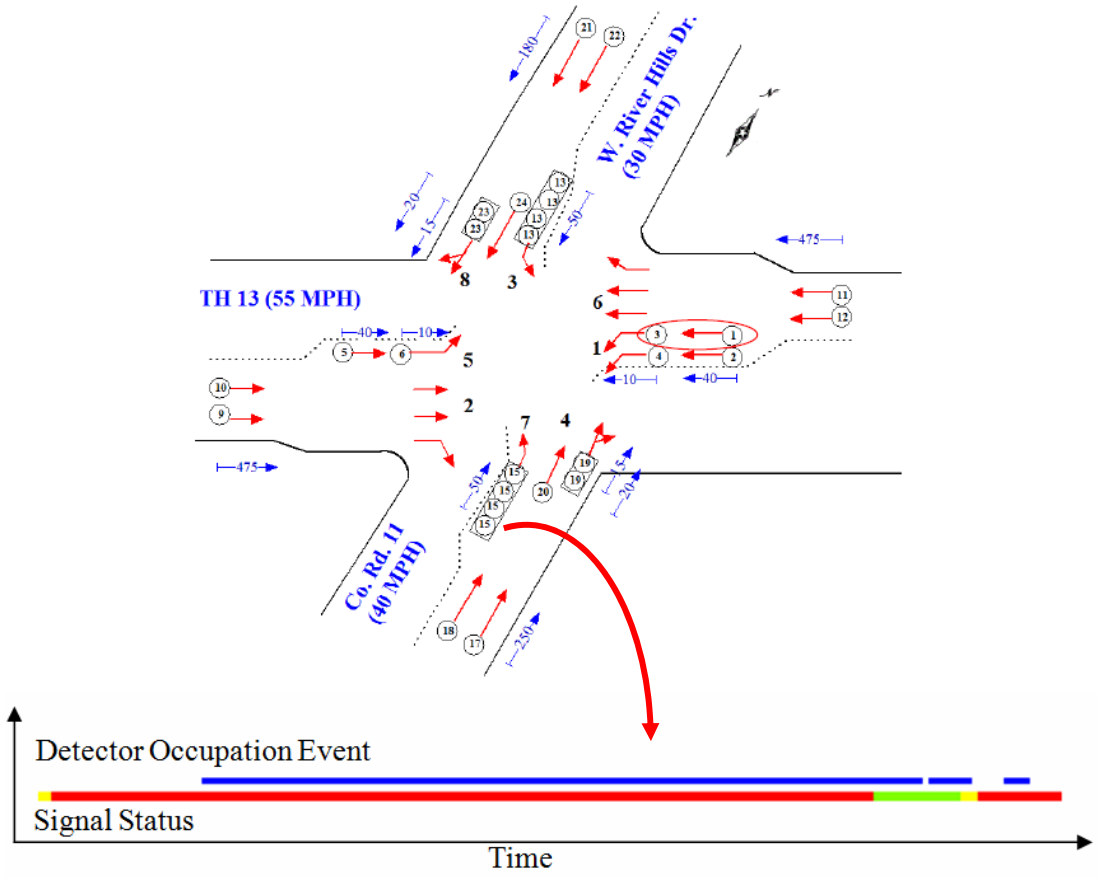

Figure 5.1 Example of traffic events from long detector at stop bar

5.1.2 Queue Service Time (QST)

Another important MOE is the Queue Service Time, defined as the length of green time

used to clear the queue (Highway Capacity Manual, 2000; Balke & Herrick, 2004). Balke & Herrick (2004) proposes to use the time elapsed from the green start to the start of first time gap identified from stop bar detector data, as the QST. This is based on the assumption that queuing vehicles will constantly place calls on stop bar detector until queue is cleared, which may not be the case if the detector is not long enough. Alternatively, we propose following formula for QST calculation. The key is to identify the end of queue departures, by identifying the first large gap from detector events. Here, a threshold gap value of 2.5 sec is used. An illustration of QST is shown in **Figure 5.2.**

$$QST_i(j) = t_{Q,i}(j) - t_{Gr,i}\ (j) \quad (5.2)$$

Where:

$QST_i(j)$ is the queue service time for phase i, for j th cycle.

$t_{Q,i}(j)$ is the end of queue departure, and is identified as the start of the first gap larger than 2.5 sec after green start, and

$t_{Gr,i}(j)$ is the start of green.

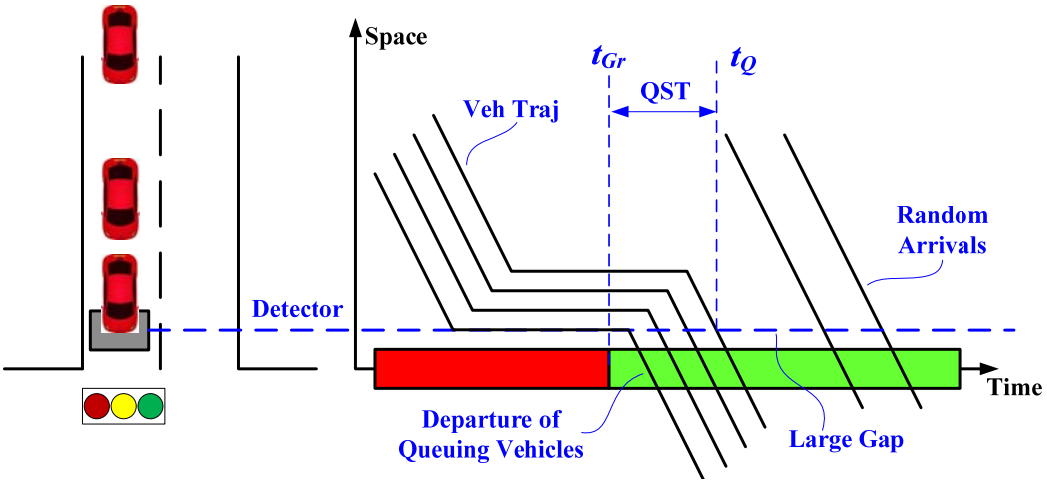

Figure 5.2 Illustration of QST

5.1.3 Utilized Green Time and Slack Green

While QST represents green time to clear the queue, it does not account for green time used by the vehicles that are not queuing. Based on the QST, the following formula is proposed to calculate the Utilized Green Time (UGT), as the total green time needed to

serve the demand within a cycle. In the formula, the first part is the QST, while the second part represents the minimum green time needed to serve the rest of arrivals.

$$UGT_i(j) = QST_i(j) + h_{s,i} \times n_i(j) \quad (5.3)$$

Where:

$UGT_i(j)$ is utilized green time at phase i, for jth cycle,

$h_{s,i}$ is the saturation headway for phase i (2 sec in our study), and

$n_i(j)$ is number of random arrivals within green time after queue is cleared, at phase i, for j th cycle.

An example of calculation of QST and UGT is shown in **Figure 5.3**. As indicated in the figure, the green start is indicated as t_A, and the end of queue departure is indicated as t_B, followed by a relatively large gap with four additional arrivals. Hence, the QST is $(t_B - t_A)$, while the UGT is $(t_B - t_A + 4 \times 2\ sec)$.

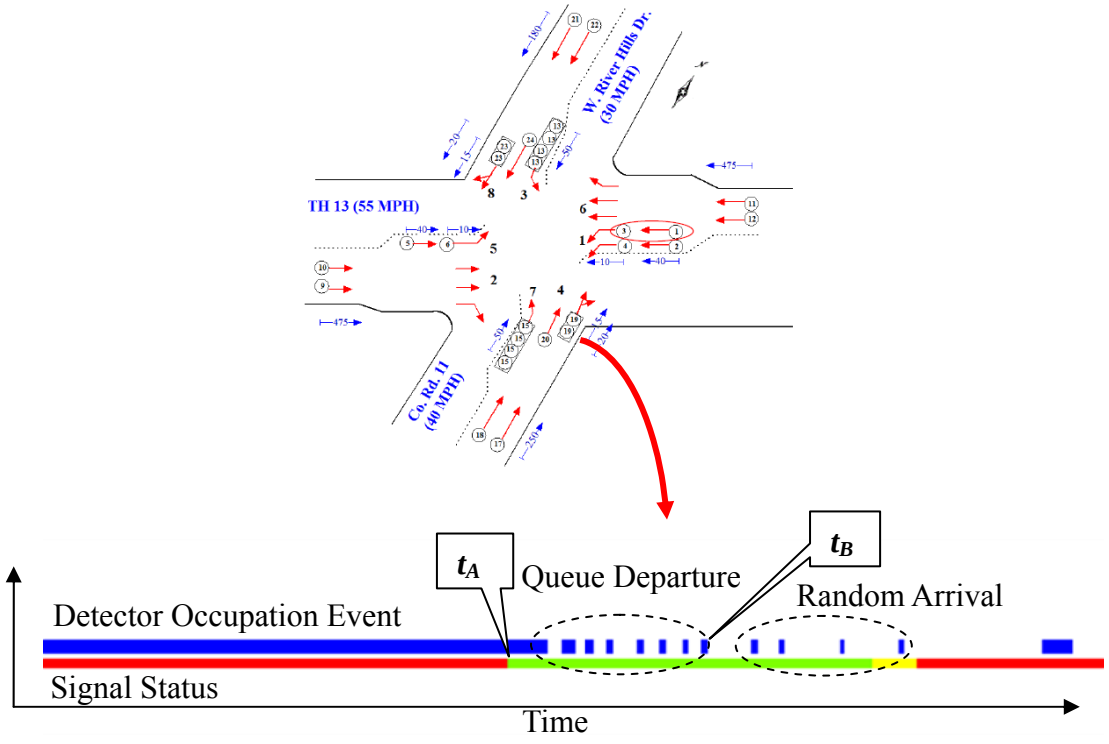

Figure 5.3 Example of QST and UGT calculation

Then, the slack green, $g_{Sl,i}$, unutilized to serve the traffic, can be calculated as:

$$g_{sl,i} = g_i - UGT_i \quad (5.4)$$

Based on the slack green, the *phase failure* can be identified for cycles without any slack green, meaning that the green time may not be sufficient to serve all the demands within one cycle.

5.2 Green splits rebalancing based on UGT

For vehicle-actuated signals, traffic engineers are typically concerned with phase failures for non-coordinated phases. Therefore, the recommended fine-tuning rule is to maintain acceptable slack green time for each phase to reduce the potential phase failures (Day et al., 2011). In addition, since the progression quality of coordinated phases is another major concern , the green splits rebalancing is restricted to non-coordinated phases only.

In addition, since NEMA controller operates the two rings concurrently, in order to compare the phase utilization across different phases, the critical phases need to be identified first. The critical phases are phases with higher green utilization, hence, smaller slack green, than the concurrent phases on the other ring. General speaking, these are relatively more congested phases. For a typical eight phase NEMA dual ring controller, following rules can be used to identify the critical phases based on the slack green, excluding the coordinated phases.

- For phase 1, 5, if $g_{sl,1} < g_{sl,5}$, phase 1 is critical phase. Otherwise, phase 5 is critical phase.
- For phase 3, 4, 7, 8, if $g_{sl,3} + g_{sl,4} < g_{sl,7} + g_{sl,8}$, then phase 3 and 4 are critical phases. Otherwise, phase 7 and phase 8 are critical phases.

Once the critical phases are identified, the splits can be first rebalanced across the critical phases. Since more slack greens exist at non-critical phases, further balancing across non-critical phases can be easily done to accommodate the changes at critical phases.

5.3 Split Fine-tuning Example

To demonstrate the split fine-tuning, an example is illustrated based on one of the

intersections on TH13. **Figure 5.4** shows the layout of the selected intersection, at Nicollet Ave & Highway 13, Burnsville. The ring-and-barrier diagram is also shown in the figure. Six phases are used with a cycle length of 130 seconds, with phase 2 and 6 as coordinated phases, and the rest phases, phase 1, 3, 4, 5, non-coordinated. The numbers on the green bars in the ring-and-barrier diagram show the max green time, plus yellow and red clearance time. The detector and signal data used were collected during 1:30 pm to 3:00 pm, from 7/08/2013 to 7/12/2013, Mon to Fri.

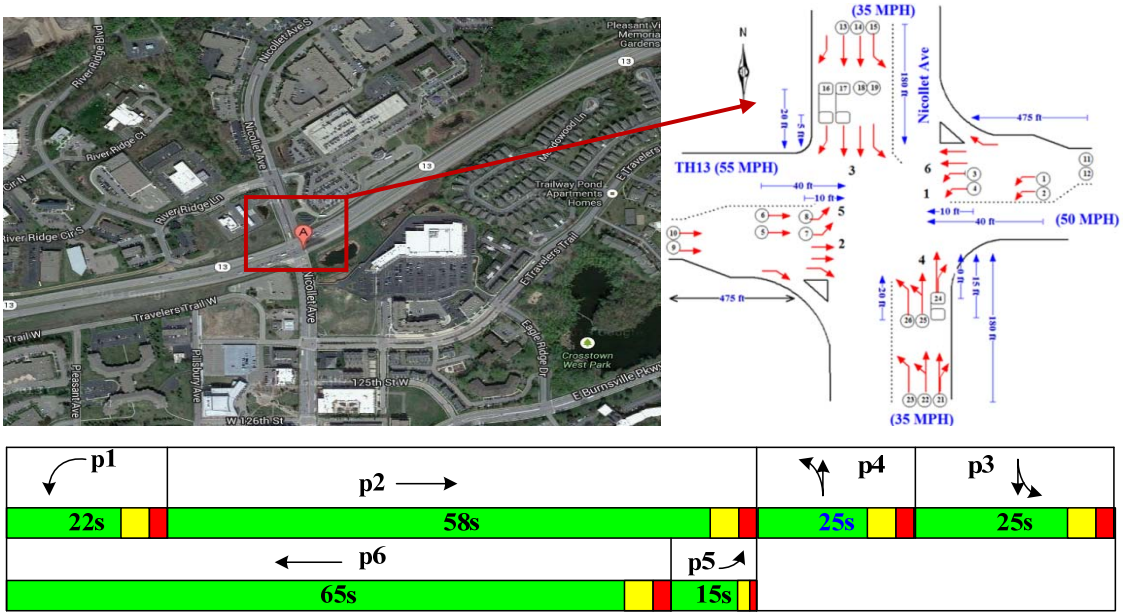

Figure 5.4 Intersection layout and ring-and-barrier diagram of the signal timing

In **Figure 5.5**, cycle-by-cycle green time with UGTs was plotted for the non-coordinated phases. The X-axis denotes the cycle index, while the Y-axis shows the length of time duration. The purple lines indicate the separation between two consecutive days. From the figure, varying green time was clearly shown at phase 1, 3, 4. Due to the fixed force off setting at coordinated phase 6, phase 5 was essentially operated as fixed-time. For phase 4 and phase 5, relatively high proportion of green have been utilized, with small slack green left, indicated by letter A. For phase 1 and phase 3, on the contrary, relatively large slack green was observed, indicated by letter B. This indicated opportunities to rebalance the green splits among the four.

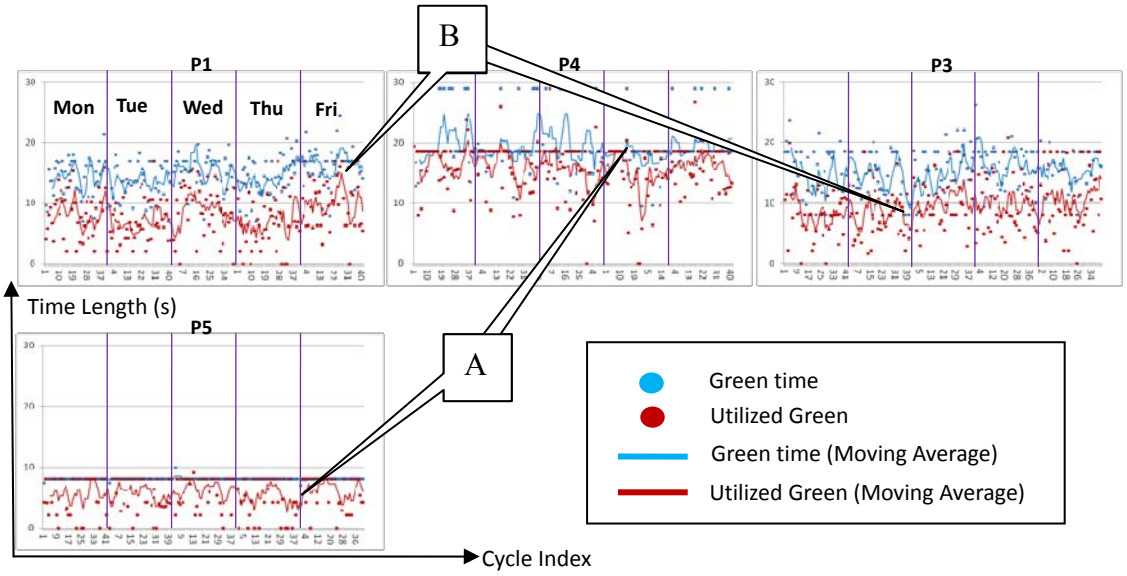

Figure 5.5 Green Time VS Utilized Green Time

After the aggregation of 5 days data, average statistics were summarized in the table in **Figure 5.6**. The information was further tabulated within the ring-and-barrier diagrams, for more intuitive interpretation. In the ring-and-barrier diagram, the green bar indicates the average green time, while the blue bar indicates the average UGT. For brevity, the yellow and red clearance signals were not plotted. The values of the UGT and green time were also denoted nearby the diagram, and were stated in the format as "Phase ID-UGT/Average Green, (Phase Failure rate)". For instance, "P3-9/15 (19%)", represents for "Phase 3 with 9 sec UGT, 15 sec Average Green, and a 19% phase failure rate".

Then, the critical phases were identified. The slack green at phase 5 was 2 sec, which was shorter than slack green at phase 1; hence, the phase 5 was the critical phase. Since no phase 7 and 8 were used, phase 4 and phase 3 were critical phases. Among the critical phases 5, 4 and 3, it would be feasible to reduce max green time for phase 3 slightly, with increase at phase 4 and 5, particularly when considering the relatively high phase failure rate with 57% and 36% at phase 5 and 4 respectively.

Table of average values for the MOEs

Phase ID	Max Green (s)	Average Green (s)	UGT (s)	Slack Green (s)	Phase Failure Rate[2]
1	17	15	8	7	3%
5[1]	10	8.0	6	2	57%
4	18.5	19	14	5	36%
3	18.5	15	9	6	19%

1: underline indicates this is a critical phase

2: phase failure rate is the proportion of cycles with phase failures

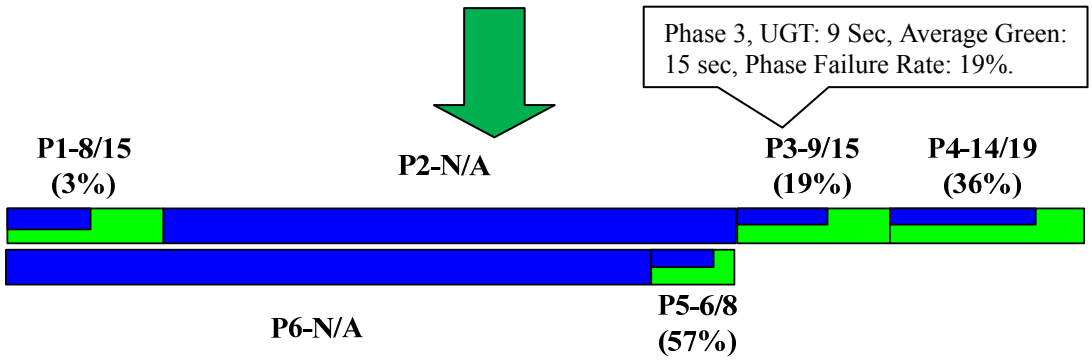

Figure 5.6 Ring-and-barrier diagrams with UGTs

CHAPTER 6 CONCLUDING REMARKS AND FUTURE RESEARCHES

6.1 Concluding Remarks

Due to the increasing needs to improve traffic management, performance measure for signalized networks has become an emerging focus in the U.S (Liu et al., 2008). However, despite of the availability of detectors, few agencies has archived or analyzed detector and signal data at signalized intersections to help signal operations. In this study, by using data collected from existing traffic signal systems, a systematic tool is successfully developed for performance visualization and fine-tuning of the arterial traffic signal system.

In details:

- To address the technical issue of data collection, DCUs were developed as a cost effective and vendor independent solution, to collect high-resolution event based traffic data.
- For the evaluation and fine-tuning of offsets, we proposed a practical procedure to construct the TS-Diagram, to visualize progression qualities of signalized arterials. Based on the data collected automatically, the TS-Diagram can be constructed periodically, without significant labor cost. The field examples were demonstrated for the proposed TS-Diagrams, and reasonable agreements were found for validation using detector data and vehicle trajectories. A field experiment was also carried out to illustrate the application of TS-Diagram for adjusting offsets and lead-lag sequence. By intuitively evaluating the TS-Diagram, changes were recommended, and a 4% reduction of total delays was achieved.
- For the evaluation and fine-tuning of green splits, an adjusted MOE, the UGT, was proposed, extended from queue service time. The ring-and-barrier diagram was adopted to tabulate the information for performance visualization and evaluation. Field examples were also illustrated to demonstrate the implementation potentials.

There are two potential applications of the signal operations in current practice that the tool can help:

(1) It can be used to validate traffic patterns and fine-tune signal parameters during signal retiming process, thus to reduce associated labor costs.

(2) It can be used to evaluate the signal performance periodically, and help engineers to identify adjustments opportunities for improvements, thus to maintain efficient signal operations over time.

6.2 Limitations and Future Researches

Limitations of the proposed approach are discussed in this section. For TS-Diagram, because traffic patterns at oversaturated intersections are not represented accurately, applications of the proposed approach to oversaturated cases should be avoided. Also, the proposed approach tends to underestimate queues and delays due to the mechanism that only data on the subject link is considered. In cases with long queues, it may be necessary to consider the upstream intersection jointly, to better evaluate the traffic conditions.

Our next step is trying to improve the accuracy of TS-Diagram by incorporating data from adjacent intersections. Other direction is to develop a more systematical approach to facilitate automated optimization of offsets, lead-lag sequence, and the green splits, using the event based traffic data. Moreover, performance evaluation and fine-tuning of cycle length and time-of-day transition schedules should also be pursued in the future.

BIBLIOGRAPHY

1. Abbas, M., Bullock, D. M., Head., L. (2001) Real-Time Offset Transitioning Algorithm for Coordinating Traffic Signals. Transportation Research Record 1748, 26–39.
2. Akcelik, R. (1994). Estimation of green times and cycle time for vehicle-actuated signals. Transportation Research Record, (1457).
3. Ahmed , A. & J. Brian (2008). An Intersection Traffic Data Collection Device Utilizing Logging Capabilities of Traffic Controllers and Current Traffic Sensors. NIATT Report Number N08-13.
4. Balke, K., & C. Herrick (2004). Potential Measures of Assessing Signal Timing Performance Using Existing Technologies. TTI Report No. 0-4422-1.
5. Balke, K., H. Charara & R. Parker. Development of a Traffic Signal Performance Measurement System (TSPMS) (2005). TTI Report No. 0-4422-2.
6. Birst, S & A. Smadi (2006). Use of Hardware-in-the Loop Traffic Simulation in a Virtual Environment," Technical Presentation at 2006 ASCE AATT.
7. Bullock, D., & A. Catarella (1998). “A Real-Time Simulation Environment for Evaluating Traffic Signal Systems”. Paper presented at the 77th Annual TRB Meeting, Washington D.C.
8. Cowan, R.J. Useful Headway Models. Transportation Research, Vol.9, No. 6, 1975, pp. 371-375.
9. Day, C. M., D. M. Bullock, & J. R. Sturdevant (2009). Cycle-Length Performance Measures: Revisiting and Extending Fundamentals. Transportation Research Record, 2128: 48-57.
10. Day, C. M., J. R. Sturdevant and D. M. Bullock (2010a). Outcome-Oriented Performance Measures for Management of Signalized Arterial Capacity. Transportation Research Record, 2192: 24–36.
11. Day, C. M., R. Haseman, H. Premachandra, T. M. Brennan, Jr., J. S. Wasson, J. R. Sturdevant, and D. M. Bullock (2010b). Evaluation of Arterial Signal Coordination. Transportation Research Record, 2192: 37–49.
12. Day, C. M., & D. M. Bullock (2011). Computational Efficiency of Alternative Algorithms for Arterial Offset Optimization. Transportation Research Record,

2259:37-47.

13. Duncan, G. (2011). Signalized Intersection Performance Measurement. In ITE 2010 Technical Conference. ITE. Accessible online: http://www.ite.org/meetings/2010TC/Session%2018%20Gary%20Duncan.pdf.Accessed on June 1st, 2013.
14. Econolite Group, Inc. (2012). ASC3 controller specification. Available online at: http://www.econolite.com/assets/pdf/controller_asc3_specification.pdf. Accessed on Aug 3rd, 2012.
15. Econolite Group, Inc. (2013). CENTRACS System Datasheet. Available online at:http://www.econolite.com/assets/pdf/systems-centracs-data-sheet.pdf. Accessed on Oct 3rd, 2013.
16. Gartner, N., & J. D. C. Little (1975). Generalized Combination Method for Area Traffic Control. Transportation Research Record, 531: 58–69.
17. Gartner, N. H., S. F. Assmann, F. Lasaga, and D. L. Hou. MULTIBAND: A Variable-Bandwidth Arterial Progression Scheme. Transportation Research Record, 1287: 212–222, 1990.
18. Gettman, D., Shelby, S. G., Head, L., Bullock, D. M., & Soyke, N. (2007). Data-driven algorithms for real-time adaptive tuning of offsets in coordinated traffic signal systems. Transportation Research Record: Journal of the Transportation Research Board, 2035(1), 1-9.
19. Gordon, R.L. & W. Tighe (2005). Traffic Control Systems Handbook. Federal Highway Administration, Report No. FHWA-HOP-06-006.
20. Gordon, R.L. (2010) Traffic Signal Retiming Practices in the United States, National Cooperative Highway Research Program (NCHRP) Synthesis 409.
21. Husch, D., & Albeck, J. (2006). Synchro Studio 7 user guide. Trafficware Ltd., Sugar Land, TX.
22. James Bonneson, Srinivasa Sunkari, & Michael Pratt (2009). Traffic Signal Operation Handbook. TxDOT. Report No. FHWA/TX-09/0-5629-P1.
23. Koonce, P., L. Rodegerdts, K. Lee, S. Quayle, S. Beaird, C. Braud, J. Bonneson, P. Tarnoff, & T. Urbanik (2008). Traffic Signal Timing Manual. FHWA. Report No. FHWA-HOP-08-024.

24. Lawrence, A. K., M. K. Mills, & D. R. P. Gibson (2006). Traffic Detector Handbook: Third Edition—Volume I. FHWA, Report No. FHWA-HRT-06-108.
25. Little, J. D. C., M. D. Kelson, & N. H. Gartner (1981). "MAXBAND: A Program for Setting Signals on Arteries and Triangular Networks," Transportation Research Record, 795:40–46.
26. Liu, H. X., Ma, W., Hu, H., Wu, X., & Yu, G. (2008). SMART-SIGNAL: Systematic Monitoring of Arterial Road Traffic Signals. In Intelligent Transportation Systems, 2008. ITSC 2008. 11th International IEEE Conference on (pp. 1061-1066). IEEE.
27. Liu, H. & W. Ma (2009). A virtual vehicle probe model for time-dependent travel time estimation on signalized arterials. Transportation Research Part C, 17 (1): 11-26.
28. Liu, H., X. Wu, W. Ma, & H. Hu (2009). Real-time queue length estimation for congested signalized intersections. Transportation Research Part C, 17 (4): 412–427.
29. Liu, H. X., J. Zheng, H. Hu, and J. Sun, Research Implementation of the SMART SIGNAL System on Trunk Highway (TH) 13. MnDOT Research Report, MN/RC2013-06. Accessible online: http://ntl.bts.gov/lib/47000/47100/47104/MnDOT2013-06_1_.pdf. Accessed on March 15, 2013.
30. Lin, F.B (1982a). Estimation of Average Phase Durations for Full-Actuated Signals.In Transportation Research Record 881, TRB, National Research Council, Washington, D.C., pp. 65–72.
31. Lin, F. B (1982b). Predictive Models of Traffic-Actuated Cycle Splits. Transportation Research, Vol. 16B, No. 5, pp. 361–372.
32. Morgan, J.T. & J.D.C. Little (1964). Synchronizing Traffic Signals for Maximal Bandwidth. Operations Research, Vol. 12, pp. 896-912.
33. National Electrical Manufacturers Association. (2003). NEMA Standards Publication TS 2. National Electrical Manufacturers Association. Rosslyn, VA.
34. National Transportation Operations Coalition. (2012). 2012 National Traffic Signal Report Card- Technical Report. National Transportation Operations Coalition. Washington, D.C.

35. Newell, G. F. (2002). A simplified car-following theory: a lower order model. Transportation Research Part B, 36(3), 195-205.
36. Petty, K., J. Kwon & A. Skabardonis (2005). A-PeMS: An Arterial Performance Measurement System. 2006 Annual Meeting Workshop. Washington, D.C.
37. Robertson, D. I. (1969). TRANSYT: a traffic network study tool.
38. Robertson, D. I., & Bretherton, R. D. (1991). Optimizing networks of traffic signals in real time-the SCOOT method. IEEE Transactions on Vehicular Technology, 40(1), 11-15.
39. Skabardonis, A. (1996). "Determination of timings in signal systems with traffic-actuated controllers." Transportation Research Record. 1554, Transportation Research Board, Washington, D.C., 18–26.
40. Smaglik, E. J., A. Sharma & D. M (2007). Bullock . Event Based Data Collection for Generating Actuated Controller Performance Measures. Transportation Research Record, 2035: 97–106.
41. Smaglik, E. J., D. M. Bullock, D. Gettman, C. M. Day, & H. Premachandra (2011). Comparison of Alternative Real-Time Performance Measures for Measuring Signal Phase Utilization and Identifying Oversaturation. Transportation Research Record 2259: 123–131.
42. Sunkari, S. R., H. A. Charara, & P. Songchitruksa (2011). A Portable Toolbox to Monitor and Evaluate Signal Operations. TTI Report No. 0-6177-1.
43. TRB (2000). Highway Capacity Manual. National Research Council, Washington, D.C.
44. Wallace, C. E., Courage, K. G., Hadi, M. A., & Gan, A. C. (1998). TRANSYT-7F user's guide. Transportation Research Center, University of Florida, Gainesville, Florida.
45. Webster, F. V. (1958). Traffic Signal Settings. TRRL Report 39. U.K. Transport and Road Research Laboratory, London.
46. Wu, X., H. Liu, & D. Gettman (2010). Identification of Oversaturated Intersections Using High-Resolution Traffic Signal Data. Transportation Research Part C, 18 (4): 626–638.
47. Wu, X. and Liu, H. (2011) A Shockwave Profile Model for Congested Urban

Arterials, Transportation Research Part B, 45(10), 1768-1786.7.

48. Yin, Y., Li, M., & Skabardonis, A. (2007). Offline Offset Refiner for Coordinated Actuated Signal Control Systems. Journal of transportation engineering, 133(7), 423-432.
49. Zhang, L., & Yin, Y. (2008). Robust synchronization of actuated signals on arterials. Transportation Research Record, 2080(1), 111-119.
50. Zhang, L., Yin, Y., & Lou, Y. (2010). Robust signal timing for arterials under day-to-day demand variations. Transportation Research Record, 2192(1), 156-166.